UNIVERSITY OF TARTU

Faculty of Science and Technology

Institute of Technology

Martin Põder

PROTOTYPE DESIGN OF ESTCUBE-2 ELECTRICAL POWER SYSTEM CONTROL ELECTRONICS

Bachelor´s Thesis (12 ECTS)

Supervisors:
Mihkel Pajusalu, PhD
Erik Ilbis, BSc

Tartu 2015

Abstract

This thesis focuses on the development of the control electronics of the electrical power system of ESTCube-2. The main goal of this thesis was to build a prototype that enhances the electrical power system of ESTCube-1 by identifying all the areas where improvements could be made and applying the solutions in the new system.

The first section of this thesis gives an overview of the scientific missions of the future satellites that are planned to be developed within the ESTCube programme. Then the control system of the electrical power system of ESTCube-1 is analysed from the hardware aspects and the requirements for the prototype are listed. The fifth paragraph focuses on the design of the prototype and gives a detailed explanation of the most important hardware and software features, as well as the functional testing results.

A fully functional prototype alongside with the low level software was achieved. The prototype features very efficient analog-to-digital converter control method, low power consumption and an input voltage failure detection mechanism. All the aimed requirements were fulfilled or exceeded. The module is easily expandable with other sections of the electrical power system to simplify the further development.

Contents

List of figures

List of tables

Acronyms and abbreviations

ADC	Analog-to-Digital Converter
BCD	Binary-Coded Decimal
CAN	Controller area network
COM	Communication system
CDHS	Command and Data Handling System
COTS	Commercial off-the-shelf
DAC	Digital-to-Analog Converter
DMA	Direct memory access
EEPROM	Electrically Erasable Programmable Read-Only Memory
eUSCI	enhanced Universal Serial Communication Interface
EPS	Electrical Power System
FIFO	First in first out
FRAM	Ferroelectric Random-Access Memory
GPIO	General Purpose Input/output
IC	Integrated Circuit
I^2C	Inter-integrated Circuit
LED	Light-emitting diode
MCU	Microcontroller Unit
MPPT	Maximum power point tracking
PCB	Printed circuit board
QFN	Quad-Flat No-leads package
RISC	Reduced instruction set computing
RTC	Real-Time Clock
SPI	Serial Peripheral Interface
SRAM	Static random-access memory
UART	Universal asynchronous receiver/transmitter
USB	Universal Serial Bus
WDT	Watchdog timer

1. Introduction

ESTCube-1 is the first Estonian satellite and it was developed within the scope of the ESTCube programme [1]. The mission of ESTCube-1 successfully reached the testing phase of the electric solar wind sail [2] components. The electron guns operated as expected and the satellite spun itself up to 840 degrees per second to unreel the tether. Only the reeling mechanism was proven to be unreliable [3]. ESTCube-1 provided valuable experience and established the infrastructure for future space projects in Estonia.

ESTCube-2 and ESTCube-3 are follow-up projects to ESTCube-1 with the main mission to reach a successful test of the electrical solar wind sail outside of the Earth´s magnetic field. The preliminary testing of the electrical solar wind sail components will be done by ESTCube-2 in the low-Earth orbit. ESTCube-2 will be a three unit CubeSat [4] and comparing to ESTCube-1, it has more solar panels to satisfy the higher power demand. Due to the increased requirements, a new electrical power system (EPS) has to be developed.

Generally, the EPS subsystem can be divided into two major sections: the control electronics and the power electronics. The control electronics part has to manage the entire EPS subsystem by conducting numerous mission critical tasks. Therefore, all its components must be developed with the utmost care, emphasizing reliability and robustness. The satellite has to operate in a severe space environment which makes the design of the satellite even more challenging.

This thesis focuses on the development of the control electronics of the EPS for ESTCube-2 with the main goals to:

- analyze ESTCube-1 EPS subsystem control electronics design from the hardware aspects to find the areas where improvements could be made;
- specify the requirements of ESTCube-2 EPS control electronics;
- built a prototype that includes improvements and complies with all requirements;
- test the performance of the prototype and its conformance to the requirements.

2. Overview

2.1. ESTCube-1

The Estonian student satellite project began in 2008 at the University of Tartu, with the main goal of educating students by providing an opportunity to build the first Estonian satellite. The collaboration between students from the University of Tartu, Estonian Aviation Academy, Tallinn University of Technology and University of Life Sciences led the successful completion of ESTCube-1 [1]. On the May 7th, 2013 the satellite was sent to low-Earth orbit with the primary mission to test the components of the electric solar wind sail [2], invented by Pekka Janhunen in Finland. [1] The reeling mechanism in the payload subsystem of ESTCube-1 had to unreel a thin conductive tether for this purpose [5]. The test was performed, but unfortunately the reeling mechanism failed due to a mechanical fault. Later investigation revealed that most probably the reeling mechanism got damaged due to the severe vibration during the launch of the rocket Vega VV02 that carried ESTCube-1.

ESTCube-1 can be considered as a great accomplishment because almost all of the goals were achieved. Firstly, it prepared the ground for future space programmes in Estonia by developing the necessary infrastructure and by providing the students with hands-on experience. Secondly, the main objective to build and launch the satellite was achieved. One of the main tasks of the satellite was to spin itself up to one rotation per second in order to unreel the e-sail tether [5]. All other subsystems stayed fully functional during the test of the spin-up. [3]

ESTCube team has already started developing follow-up projects to ESTCube-1. The concept of the future satellites is to test the e-sail on a bigger scale and in the real environment which is somewhere outside of the Earth´s magnetic field, for instance in the lunar orbit. ESTCube-3 is planned to be equipped with cold gas thrusters for attitude and orbit control purposes, deployable solar panels to satisfy the increased power demand and the e-sail tether to perform the scientific experiment. The main purpose of ESTCube-2 is to test the e-sail components and other subsystems used in ESTCube-3 in the low-Earth orbit. Satellite launches to the orbits where ESTCube-3 can accomplish its mission are expensive and arranged infrequently. Therefore ESTCube-2 must test the eligibility of the technology to increase the probability of success of ESTCube-3.

2.2. Overview of the EPS control electronics designs

The electrical power system (EPS) is one of the most important subsystems of every satellite. It has to accomplish numerous critical tasks including energy harvesting, battery charging, providing electrical supply to all other subsystems and logging data in order to provide statistics of power production and consumption.

There are two commonly used approaches in the way the EPS is controlled within the satellite. Firstly, the EPS can be controlled by the satellite´s main microcontroller unit (MCU). This approach reduces the complexity of the EPS, but burdens the main MCU with time consuming monitoring and logging operations.

Second way of controlling the EPS is by using a dedicated MCU that accomplishes all the necessary tasks for the EPS to function. These tasks can be interacting with other subsystems, monitoring and logging power harvesting and consumption, switching on and off the supply voltage of other subsystems and handling the maximum power point tracking (MPPT) algorithm. Since the EPS stays constantly operational and some of its tasks, like logging, are done frequently, the EPS MCU should have low power consumption to reduce the overall power demand of the satellite.

The Norwegian satellite CubeSTAR uses dedicated MCU ATxmega128A1 from Atmel as a dedicated EPS control MCU. The MCU is used for implementing the MPPT algorithm for charging the batteries and it also provides the telemetry data. The MCU is connected with the satellite´s main MCU via an inter-integrated circuit (I^2C) bus. [6]

AAUSAT3, the third Danish CubeSat, uses a dedicated MCU AT90CAN128 (Atmel) for controlling battery charging and discharging, monitoring general health of the satellite, and organizing the power distribution. The MCU is connected to the other subsystems through a controller area network (CAN) bus. [7]

The EPS design of the student satellite OUFTI-1, developed in the University of Liege, does not have a dedicated MCU. The EPS printed circuit board (PCB) contains two analog-to-digital converters (ADC) ADS7830IP (Texas Instruments) and MAX1039 (Maxim

Integrated). The ADCs are connected with the on-board data handling subsystems via I^2C bus and they are used for measuring currents, temperatures and bus voltages. [8]

The EPS subsystem of NUTS-1, a 2-unit CubeSat from Norwegian University of Science and Technology, does not have a MCU either. The EPS utilizes INA219 (Texas Instruments) I^2C current and power monitor integrated circuits (IC) that are controlled by the on-board controller module as well as by the telemetry, tracking and control module. [9]

2.3. Electrical power system control electronics of ESTCube-1

The EPS of ESTCube-1 is controlled by a dedicated MCU that is responsible for power distribution, collecting and logging telemetry data and controlling the bacon signal. Figure 1 shows the block diagram of the EPS control electronics of ESTCube-1.

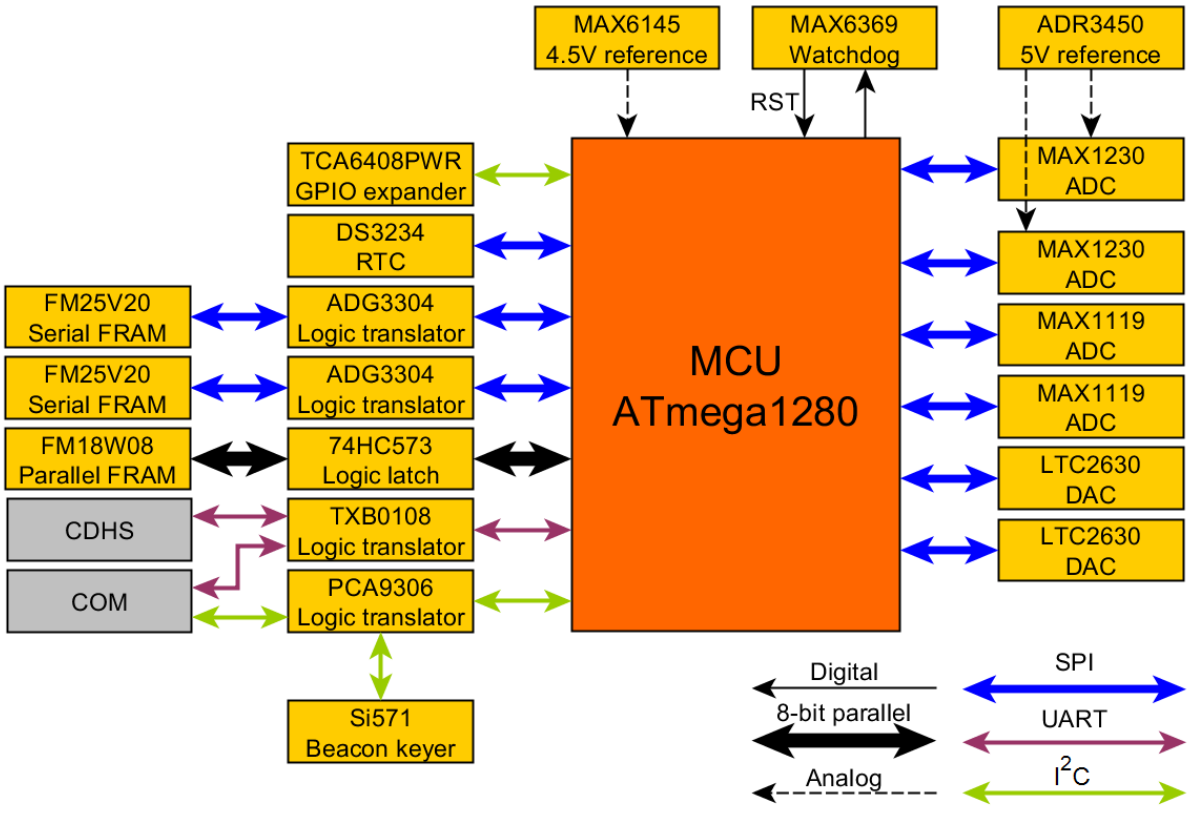

Figure 1: The EPS control electronics of ESTCube-1 [12].

2.3.1. Design analysis of the EPS control electronics of ESTCube-1

ESTCube-1 EPS is based on an 8-bit MCU ATmega1280 from Atmel, which has 128 KB of program flash, 4 KB of electrically erasable programmable read-only memory (EEPROM), 8 KB static random-access memory (SRAM) and a 10-bit ADC with 16 inputs [10]. This MCU was chosen for this application because it has low power consumption, 86 general purpose input and output (GPIO) pins [10], it has been tested for radiation [11] and it had previous flight heritage. [12]

An external watchdog timer (WDT) MAX6369 (Maxim Integrated) is used instead of the MCUs internal WDT to provide flexible and independent timeout settings. The MAX6369 enables to set seven different timeout periods within the range from 1 millisecond to 60 seconds in the hardware, using pull-up or pull-down resistors [13]. ATmega1280s internal WDT timeout can be varied only from 16 milliseconds to 8 seconds [10].

The microcontroller is connected to two types of ferroelectric random-access memory (FRAM) chips. The 32 KB parallel FRAM memory FM18W08 (Cypress) is used to expand the MCU´s random access memory and two serial 2 Mbit FM25V20 (Cypress) FRAM memories are used for the measurement data and firmware image storage. [12]

All necessary measurements are performed using the MCU´s internal 10-bit ADC as well as standalone ADCs. The MCUs internal ADC uses a 4.5 V reference voltage source MAX6145 (Maxim Integrated). Two 16-channel 12-bit external ADCs MAX1230 obtain their 5 V reference voltage from ADR3450 (Analog Devices). Battery temperature acquiring and backup measurements of the main power bus voltage are performed by two 8-bit ADCs MAX1119 (Maxim Integrated) with internal 4.096 V reference source. The system is capable of measuring the main power bus voltage with three different ADCs (MAX1119, MAX1230 and ATmega1280 internal ADC). This feature allows comparing the results in order to detect degradation of the ADCs. [12]

One of the tasks of the EPS is keeping the date and time of the satellite [12]. DS3234 (Maxim Integrated) is used for this purpose due to its accuracy and thermal stability. It features

internal temperature compensated crystal oscillator ensuring time precision of ±3.5 ppm in the temperature range of -40 °C to 85 °C [14].

2.3.2. Areas of improvements of the EPS of ESTCube-1

The EPS subsystem together with the MCU operates at 5 V voltage, while the serial mass storage FRAM memories operate at 3.3 V. This difference in voltages requires for a transition in the logic levels. An ADG3304 (Analog Devices) is used to interface the lower voltage FRAMs with the MCU. Since all other subsystems in ESTCube-1 work on 3.3 V, logic level translators are required to communicate with them. TXB0108 (Texas Instruments) and PCA9306 (Texas Instruments) are connected to universal asynchronous receiver/transmitter (UART) and I^2C buses which are providing vital communication interface to the command and data handling system (CDHS) and communication system (COM). [12]

These logic level translators between mission critical peripherals and subsystem´s communication buses reduce overall system reliability. In the case of failure, they might have a severe impact on the functionality of the satellite.

A simple solution would be to adopt components with working voltage of 3.3 V in the entire subsystem. This resolves the previously mentioned reliability issue by eliminating all the logic level translators as well as reducing overall current consumption and component count.

The EPS of ESTCube-1 has a capacitor bank to ensure short time (80 milliseconds [12]) operation of the subsystem when the voltage on the main power bus suddenly disappears. This time can be used to pinpoint the fault, save it to a log and to try to restore the power to the system. The loss of the voltage can be detected only with the ADC during routine logging measurements. [12] The problem of this approach is the latency between the actual occurrence and the discovery of the fault.

An ideal solution would notify the MCU with an external interrupt as soon as the voltage has decreased below a certain threshold. A separate, fast and reliable fault detection circuitry must be developed in order to achieve this.

ESTCube-1 EPS subsystem has to measure 48 analog voltages during one routine logging acquisition [12]. Due to the inefficient method of controlling the ADCs, the time it takes to measure all 48 channels is 5 milliseconds [3]. When measuring rapidly changing currents, this long measurement window can result in miscalculations because the acquired results do not describe the same moment in time.

Another issue is that the MAX1230 ADCs are used in a mode where acquisitions are initiated one at a time by sending a command byte to the ADC [12]. Since the serial peripheral interface (SPI) clock signal is used to clock the ADC conversions, the MCU must conduct the whole measurement process. Should an external interrupt occur during a multichannel acquisition, the measurement process is suspended for undefined amount of time. This can lead to unpredictable timing errors between several sequential ADC measurements. The problem evolves further with the increase of total channels to be measured in series.

These problems can be approached in two ways, either by using dedicated sample-and-hold circuits for every input channel of the ADC, or by controlling the ADCs in a more efficient way. First approach means that all channels would be sampled simultaneously and then measured separately from the sample-and-hold IC outputs. This would definitely solve the problem, but in the other hand it would increase the count of components by the number of necessary analog inputs and therefore make the design more complex and less robust. The more efficient method for controlling the ADCs can utilize the ADCs internal first in first out (FIFO) memory and oscillator in order to perform acquisitions autonomously. This can be achieved with no extra hardware but it would only reduce the severity of the problem, not solve it entirely.

The power consumption of the EPS control electronics can be also viewed as an area of improvement. Since the EPS is constantly operational, its idle power consumption should be as little as possible. Therefore, the power consumption should be important criteria when choosing the components of the new design. The energy that can be saved would definitely have a better utilization, for instance, it can be used for charging the batteries.

3. System requirements

The requirements for the EPS control electronics of ESTCube-2 are following:

- a supply voltage of 3.3 V;
- active mode power consumption less than 30 mW;
- 30 12-bit external ADC channels with measurement time window less than 500 µsec. The number of input channels should be easily expandable;
- a voltage fault detection system including capacity bank, that holds the MCU operational at least 100 ms after the input voltage failure;
- at least 60 MCU GPIOs for peripheral devices;
- MCU with at least 64 kB of internal FRAM memory;
- at least 4 Mbit of external FRAM memory;
- an real-time clock (RTC) with temperature compensated crystal oscillator and accuracy better than ±5 ppm;
- two half-duplex RS485 UART channels for connecting the EPS with the satellite´s communication bus;
- all components with radiation testing and previous flight history are preferred.

Since the aim of this thesis is to build a prototype that must be easily debuggable and customizable, a few extra requirements were set to the prototype:

- a 3.3 V voltage regulator for powering the platform from the universal serial bus (USB) port;
- pin headers between the main supply and individual sections supply lines for measuring current consumption and for disabling individual devices;
- debugging light-emitting diodes (LED) connected to the free GPIO pins of the MCU;
- test points for all critical signals to enable convenient oscilloscope probing;
- pin headers for the inputs and outputs of all peripheral devices.

3.1. Requirements for the electronic components

Dedicated space grade components are expensive, bulky and not easily available. Therefore all the electronic components used in this project should be commercial off-the-shelf (COTS).

Quad-flat no-leads packages (QFN) are preferred due to their size, thermal performance and mechanical robustness. In the near vacuum environment, there is no heat convection so thermal energy is transported only with conductivity and dissipated with thermal radiation. Consequently, low thermal resistance between components and the PCB has to be priority. QFN packages, for instance, have a large thermal pad to increase the heat transfer to the PCB.

Integrated circuits using an SPI interface are recommended because SPI is simple, enables full duplex connection at high clock speeds and can be easily debugged compared to the UART and I^2C. The SPI implementation in hardware does not have a flow control and it is based on shift registers [15]. This simplifies the software and makes the overall design more robust. Moreover, the SPI is ideal for transferring large amounts of data so it is very suitable for accessing the memories.

4. Materials and methods

Altium Designer 14 was used for the schematic and the PCB design. It was chosen to ensure compatibility with other sections of the EPS subsystem. Altium Designer will be used throughout the design process of ESTCube-2.

Texas Instruments LaunchPad MSP430FR5969 Evaluation Kit was used in order to flash the software onto the MCU. The board includes:

- One MSP430FR5969 MCU with buttons, LEDs and pin headers for external circuitry;
- a USB emulator for programming and debugging the on-board MCU as well as an MSP430FR series external MCU via Spy-Bi-Wire interface [16];
- an USB to UART channel, enabling virtual serial port communication between the MCU and the computer. [17]

The freeware version of Code Composer Studio 6.0.1 was used for software development and debugging. This Eclipse framework based integrated development environment has 16 kB firmware size limit which is enough for preliminary testing. The software included plenty of code samples that made the studying of the previously unfamiliar MCU very easy.

An Agilent MSOX4054A digital oscilloscope was used for debugging and testing purposes. All current and voltage measurements were taken with a Tektronix DMM4050 precision multimeter.

5. Results and testing

5.1. Overview

A complete EPS control electronics prototype was designed, assembled and tested. The prototype has two MCUs, one for subsystem control, and other for diagnostics purpose. In order to increase reliability, the main MCU can take over controlling the ADCs at any time using bus switch. The block diagram of the prototype is shown on Figure 2.

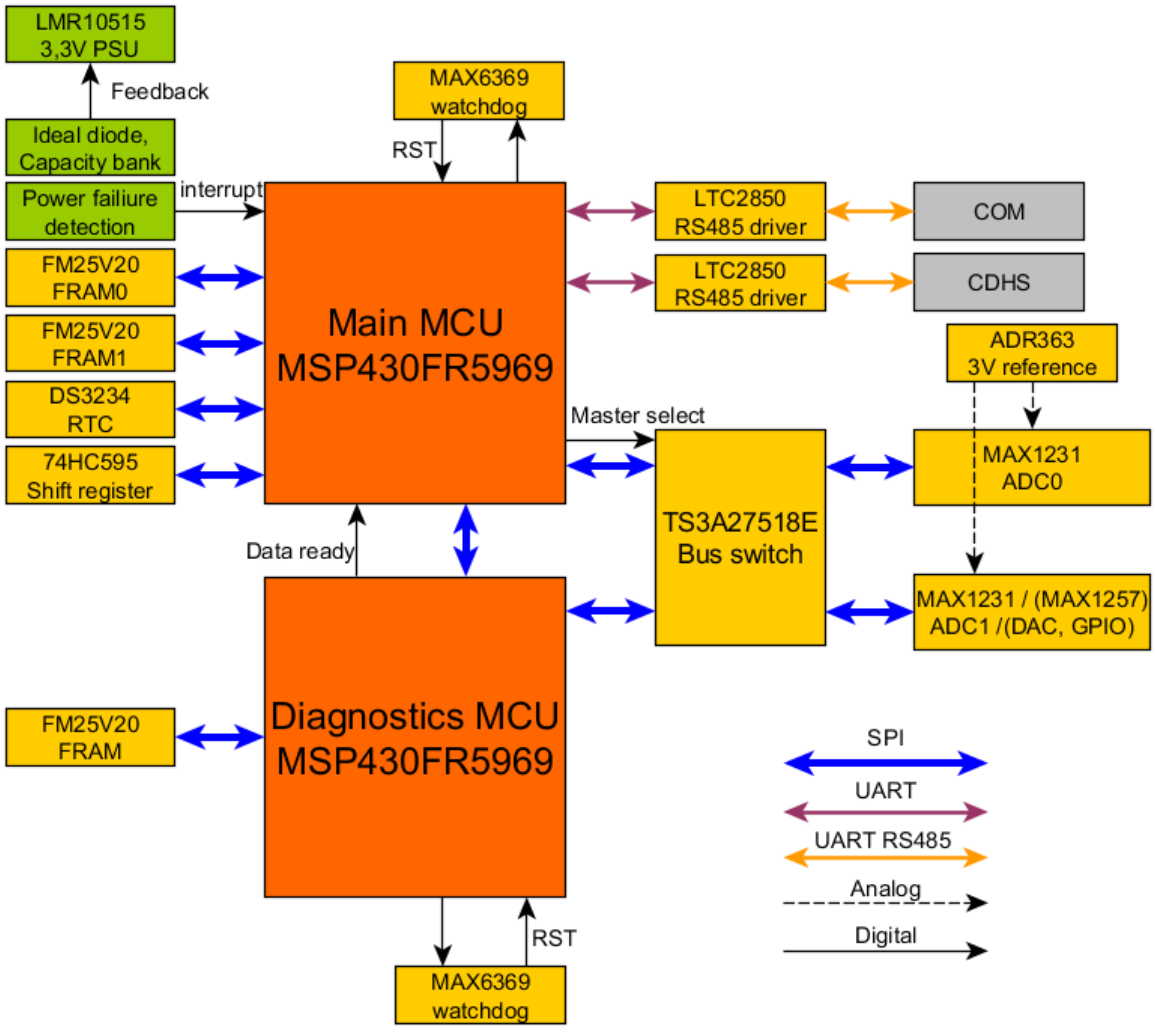

Figure 2: Block diagram of the electrical power supply control electronics prototype design.

The prototype includes lots of pin headers for connecting external devices, test pins for convenient oscilloscope probing, debugging LEDs with common ground connected to pin header, and switching voltage regulator in order to supply the prototype from a USB port. Pin headers, shown on Figure 3 with red jumpers attached, were added into the power paths of every functional section to enable separate current measurements.

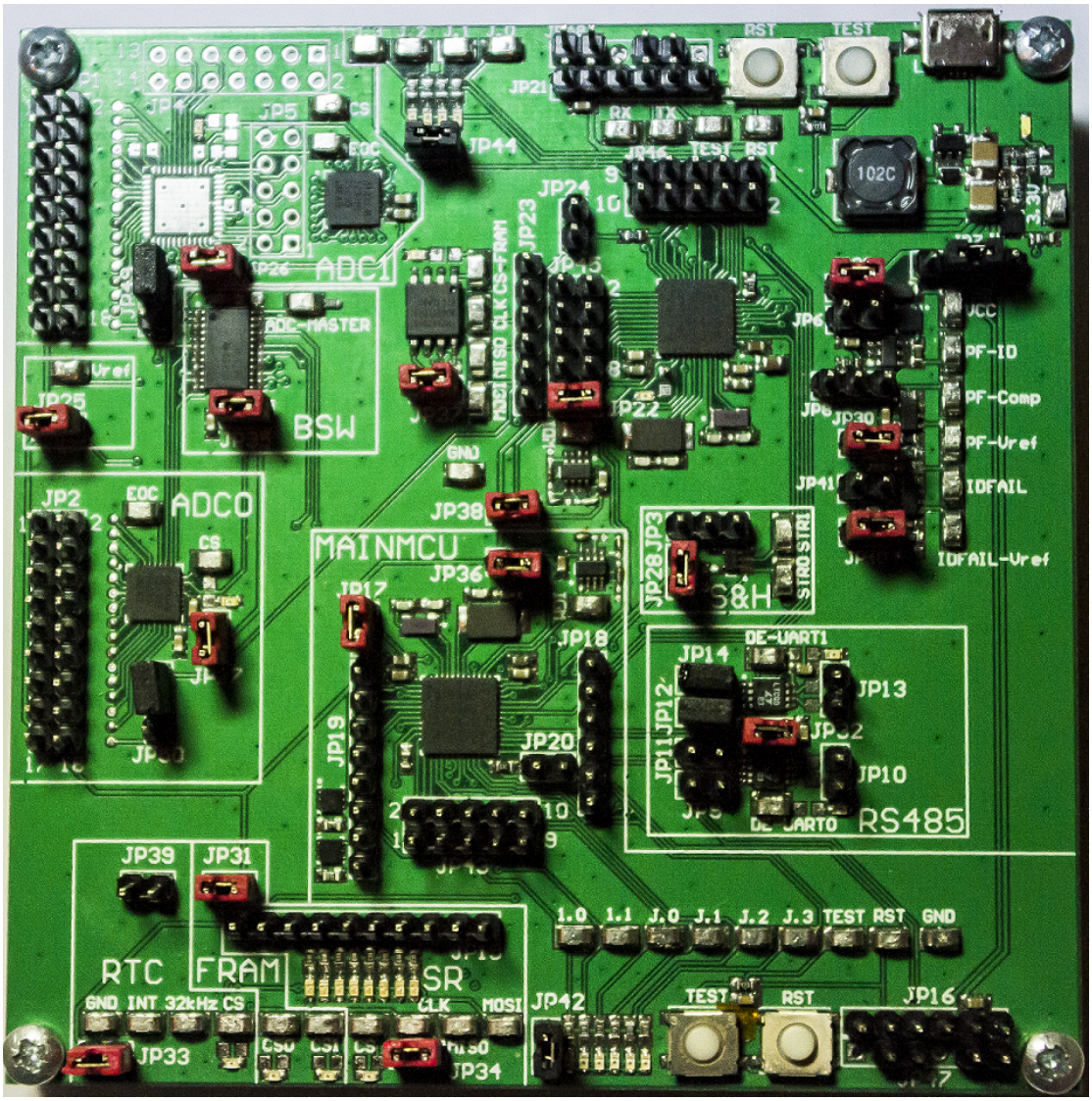

Figure 3: Picture from the top of the assembled prototype.

Figure 4 views the back side of the prototype. In order to simplify the usage of the board, a description of every pin header was added to the bottom silkscreen layer, as well as the pinout to the top silkscreen.

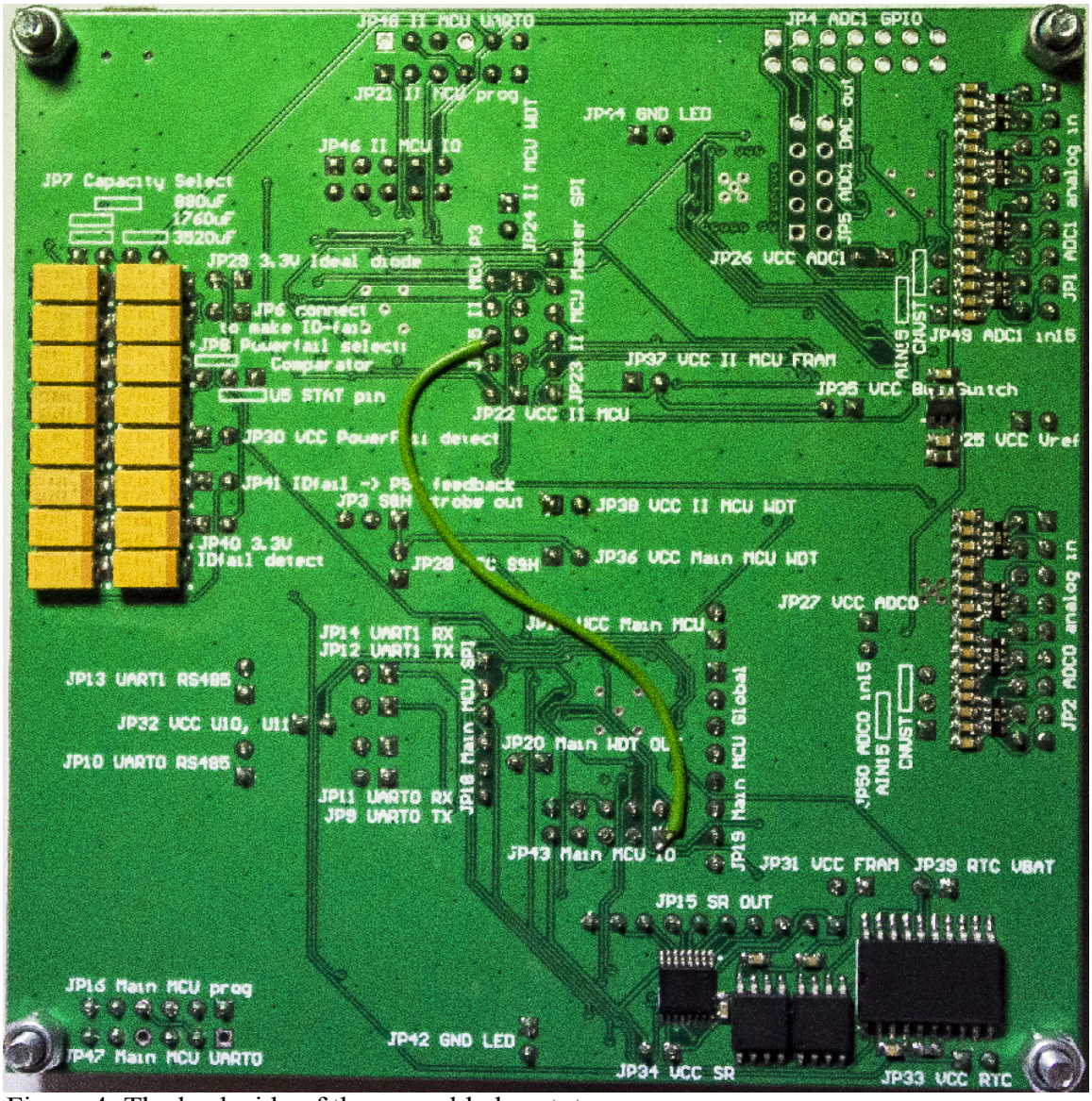

Figure 4: The back side of the assembled prototype.

5.2. Hardware design based on 3.3 V supply voltage

In order to remove all the logic level translators from the design, some components from the EPS of ESTCube-1 were replaced in the new design. The MCU was the starting point of selecting new components.

MSP430FR5969 is a 16-bit reduced instruction set computing (RISC) architecture based MCU featuring 1.8 to 3.6 V supply voltage, 100 µA/MHz active mode current consumption, 40 GPIOs, dual frequency clock system using separate crystal oscillator inputs and three

enhanced Universal Serial Communication Interfaces (eUSCI) supporting UART, SPI and I^2C buses. In addition, this particular MCU includes 64 kB of FRAM that can be used for program memory as well as for random access memory. The FRAM is deployed in the software equally as traditional SRAM. This MCU suits ideally for this application, since the FRAM´s non-volatile manner enables the storage of a mission critical data inside the MCU. Moreover, FRAM´s high tolerance towards ionizing radiation increases the endurance of the MCU [18].

Two MSP430FR5969 (Texas Instruments) were integrated to the design mainly to fulfil the GPIO and program memory requirements but also to enable separated parallel threads that could be useful for controlling the ADCs more efficiently. The second MCU (hereafter called as diagnostics MCU) was planned to control the ADCs and to log data. Its purpose besides fulfilling the main requirements is to release the main MCU from time consuming data logging, thereby enhancing the ADC measuring method problem that occurred on ESTCube-1 EPS. Both MCUs work at 8 MHz and communicate via SPI bus.

At the time of choosing the components, the MSP430FR5969 had the largest internal FRAM among all available MCUs. About seven months later when all the practical work was already finished, a better MCU became available. The MSP430FR6989 has 128 KB of FRAM, 83 GPIOs, and 4 eUSCI modules [19]. This particular MCU satisfies all the requirements but the decision whether to eliminate the second MCU from the next version of the EPS subsystem needs further analysis because the design based on two MCUs has its own advantages and disadvantages over the solution with a single MCU.

The MSP430 series MCUs have been previously tested for ionizing radiation. A TelosB wireless sensor node, containing a MSP430F1611 [20], stayed fully functional during the radiation test in which it received a dose of 30 krad. After a 48 hour of annealing, it failed to be reprogrammed with new firmware. [21] As this MCU used ordinary flash memory for firmware storage, the MCU with internal FRAM may be more reliable.

The same family MCU used in this project, MSP430FR5739, was used on-board ESTCube-1 to control the piezoelectric motor which unreels the electric solar wind sail tether. [22]

Both MCUs used in the prototype are connected with two different frequency crystals. One 8 MHz for sourcing active mode clock and second 32.768 kHz for RTC operations. MSP430FR5969 supports a maximum clock frequency of 16 MHz, whereas the FRAM

maximum access speed is limited to 8 MHz. Wait-states are required for FRAM access if the MCU works at higher clock speeds than 8 MHz [23].

The MCUs continued using external watchdog timers MAX6369 (Maxim Integrated), as they work at 3.3 V, have robust wide range (1 ms to 60 s) timeout setting functionality via hardware and have open drain output, which is necessary for the Spy-bi-wire communication with the MCU [13]. MAX6369 are intended to provide a short runtime watchdog functionality to recover from the MCU software faults. The MCU´s internal watchdog timer, which timeout period can have 8 different values from the range from 1.95 ms to about 18[1] hours [24], is used as a dedicated watchdog for hard resetting[2] the satellite.

[1] 18:12:16, when sourcing the watchdog clock from 32,768 kHz crystal.
[2] Hard reset causes a power cycle to the whole satellite by disabling battery discharge and waiting for the satellite to enter umbra.

5.3. The input voltage fault detection with capacitor bank

The input voltage fault detection was implemented in two ways to test which of them operates better. First presumption was that it can be achieved with no extra hardware, using the power path controller IC LTC4412 (Linear Technology) which is already integrated into the incoming supply circuit in order to provide ideal diode functionality. This IC has an open drain status output that is activated when the voltage at the sense pin is 20 mV higher than the input voltage [25]. This solution suits for detecting the fault, but it lacks the opportunity to change the 20 mV threshold voltage. Figure 5 shows the schematic of the implementation.

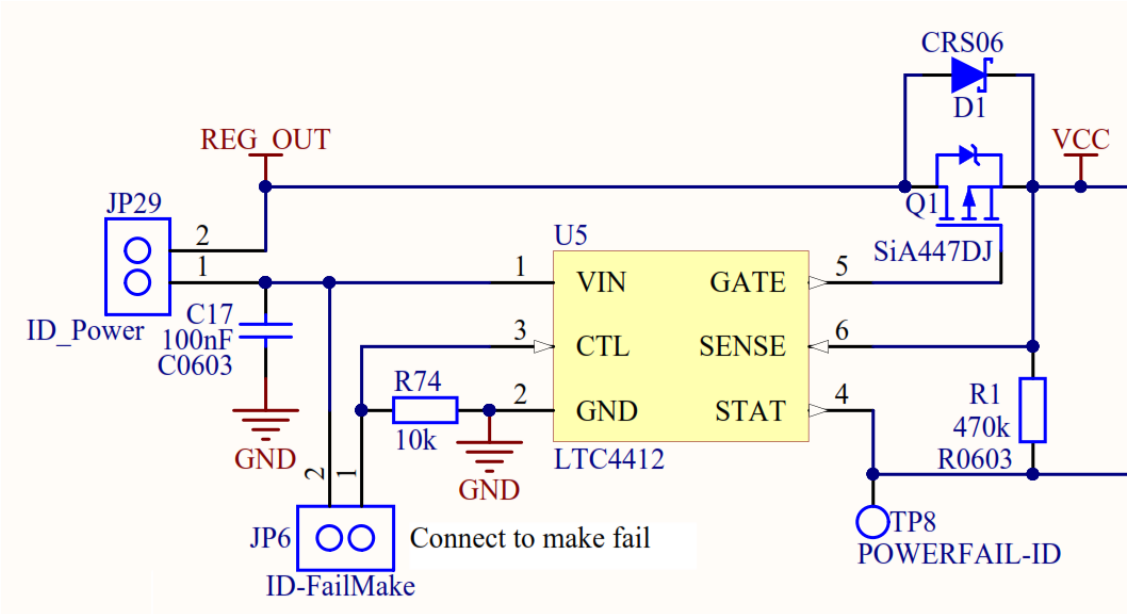

Figure 5: Input voltage fault detection circuit based on LTC4412 power path controller.

In order to set a custom threshold voltage, a solution based on a Schmitt trigger was implemented. The circuit shown on Figure 6 consists of a comparator LMV7271 (Texas Instruments) and feedback resistors. In a normal condition, the output of the comparator is low [26] and therefore R78 and R79 make up a voltage divider that sets the comparator threshold at about 115 mV below the VCC. When the supply input voltage from the REG OUT line, fed to the inverting input, falls below the threshold, the output of the LMV7271 goes high and this is registered in the MCU as an external interrupt. When the output is high, R78 and R79 are both at the potential of the VCC and consequently the threshold is set to the voltage of VCC. In this case the REG OUT has to rise above the VCC to restore the low state

of the comparator output. The JP30 is added to the supply line to enable measuring the current and isolating the IC from the VCC.

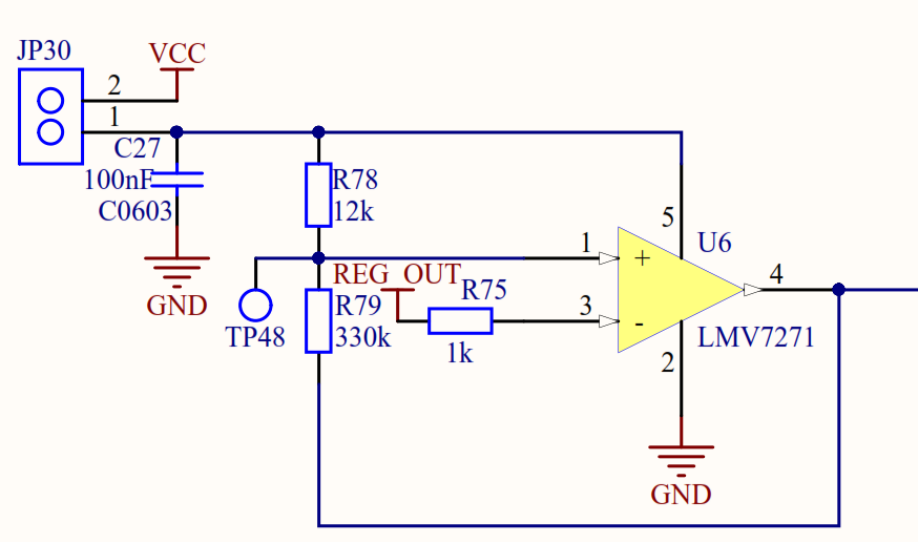

Figure 6: Input voltage fault detection circuit based on a comparator.

When the supply voltage suddenly disappears from the REG OUT, MCU and its peripherals are supplied from a tantalum capacitor bank tied to the VCC rail. To conveniently change the capacity during testing, the bank was divided into two blocks of 1760 µF, each connected to the pin headers. This enables the selection of the capacity of 880 µF, 1760 µF and 3520 µF by connecting the blocks in parallel or in series. This feature is implemented only in the prototype PCB. The flight version of the EPS will contain a capacitor bank with fixed capacity.

The time diagram in the Figure 7 describes the test results of both methods discussed above. The test was carried out with capacitor bank of 880 µF, supply voltage of 3.3 V and by unplugging the USB cable that supplied the on-board switching regulator with 5 V. The MCU was programmed to transmit random data to the serial port in order to detect how long it stays operational. The test showed that both methods accomplish the task, but as the version with standalone comparator can be made more tolerant of false alarms generated by the interference in the supply line, this solution is preferred.

It can be seen from the oscilloscope screen capture (Figure 7) that the MCU shuts down precisely at 1.8 V, as the datasheet specifies [23] and is operational about 206 ms after both powerfail interrupts occurred. The time difference between two detection methods was measured roughly 1 ms, which is negligible.

Figure 7: Test results of the input voltage fault detection methods captured with an oscilloscope.

5.4. External analog-to-digital converters

Other significant components to be changed were the ADCs, as they were working on 5 V supply voltage. The MAX1230, used in ESTCube-1 EPS, was replaced with MAX1231. Both these ADCs are produced by Maxim Integrated and differ only in supply voltage. This simplifies the new design, especially from the firmware perspective. When examining the datasheet of MAX1231, it turned out that one of its analog inputs has an alternative function of providing capability to trigger conversions [27]. So instead of writing command byte via the SPI bus, one can simply put this input low for at least 1.4 µsec to start a predefined acquisition cycle. The ADC then performs measurements using its internal 4.4 MHz clock,

writes results to its 34-byte FIFO and puts end of conversion output low [27]. This is registered as an external interrupt event in the MCU, indicating that SPI data transaction can commence. Then the data from the ADC FIFO is read into the MCU. The conversion time of 15 channels using this method is 70 μsec[3].

This method is significantly better for controlling these ADCs, because the MCU does not have to intervene in the acquisition process. Furthermore, as the trigger signals can be dispatched simultaneously to multiple ADCs, this minimizes the time gap between sequential input channels of different ADCs. It also enables to increment the number of ADCs with no increase in acquisition time.

Another feature involved with the ADCs was to provide compatibility to MAX1257, which integrates 16-channel 12-bit ADC, 8-channel digital-to-analog converter (DAC) and 12 GPIO into a single miniature 48-pin QFN package [28]. This highly functional IC could lose the need for external DACs used for giving feedback to voltage regulators in the ESTCube-1 EPS [12]. Unfortunately, the availability of this IC was problematic during the design phase, so one ADC circuitry was made to support both, MAX1231 and MAX1257 footprints. This enables the opportunity to test MAX1257 in the future, should the need for it arise.

The whole system´s supply voltage was reduced from 5 V to 3.3 V hence the ADCs reference voltage source had to be replaced. ADR363B from Analog Devices was chosen since it provides 3 V output with ±3 mV accuracy, has fractional 9 ppm/°C temperature coefficient and is specified to work in a temperature range from -40 °C to +125 °C [29].

To provide both MCUs with the ability to control the ADCs, a 6-channel multiplexer TS3A27518E is used as SPI bus switch. The main MCU decides which MCU controls the ADCs by setting or clearing one digital output.

[3] MAX1231 using external reference, without averaging and temperature request, measured from the falling edge of conversion start signal to the falling edge of the end of conversion signal.

5.5. MCU Software

Since plenty of peripherals stayed consistent, some low level logic and frontend code from ESTCube-1 EPS was reusable. However, the entire processor specific driver layer had to be developed from scratch. This section describes the most important parts of the software that make up a small amount of the whole software that was written within the scope of this thesis.

5.5.1. Improved external real-time clock DS3234 driver

The time and date in DS3234 real-time clock is stored in binary-coded decimal (BCD) [14], whereas the MCU time structure is using ordinary 8-bit unsigned integer format. On the EPS of ESTCube-1 the conversions between the two formats were implemented in the software. It was based on lots of arithmetic including dividing, which resulted in relatively slow process. The new driver version utilizes a special decimal to BCD and BCD to decimal hardware conversion registers that are included in the MCU RTC module [24]. Driver software simply writes to these registers in one format and reads another. This makes the driver very fast and efficient.

5.5.2. Data connection between main- and diagnostics MCU

The communications between two microcontrollers is based on SPI because it enables full duplex connection at high speeds, in our case 4 MHz. The master of the SPI bus is the main MCU and data transactions are initiated with a command byte sent by the main MCU. The diagnostics MCU sets data ready output, indicating that it is ready for the transaction. Depending on the specific command, data can be received, transmitted or swapped. Due to the high clock speed of the SPI bus, advanced techniques must be used for the diagnostics MCU SPI logic. If the diagnostics MCU is not capable of reading or writing SPI shift registers fast enough, erroneous data could be transferred.

Direct memory access (DMA) provides a splendid solution to this problem. With DMA, the data can be moved between two software defined memory locations without the MCU intervening. The software must specify transmit and receive memory addresses, byte count, transaction trigger event and enable the DMA channel. After that, the DMA controller starts

data transfer and the MCU can continue with other tasks, for instance processing the next command. The transfer of one byte takes usually only few[4] clock cycles.

This method was applied to the diagnostics MCU´s driver software. Three types of communications were implemented: sending, receiving and swapping. The full-duplex nature of SPI was utilized by giving the opportunity to dispatch a new command to the diagnostics MCU while it is sending data to the main MCU. Since all data transactions in the diagnostics MCU are implemented with DMA, this gives a chance to process commands during the transactions. A double buffering was added to the transmit channel of the DMA so that data could not be modified during transmissions.

An example program, described on Figure 8, was developed to both MCUs demonstrating the data link in operation.

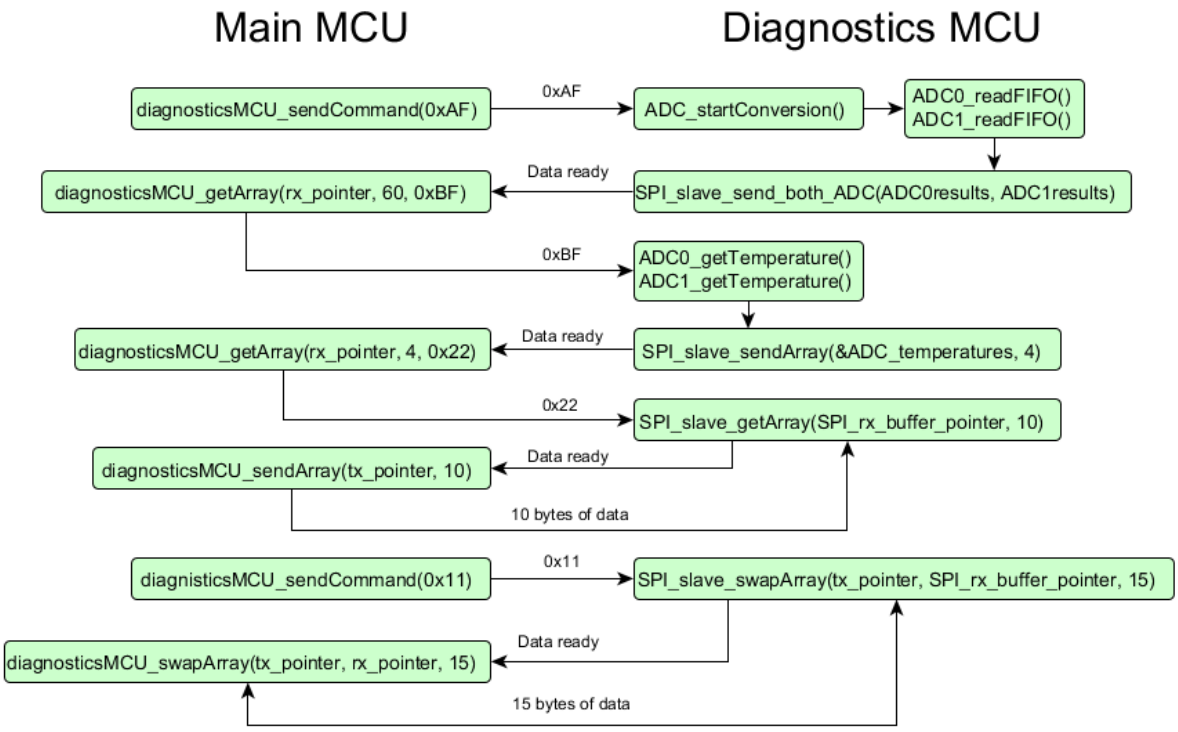

Figure 8: The software logic of the two MCUs doing various types of data transactions during example program execution.

[4] MSP430FR5969 in active mode: 4 cycles [24].

The Figure 9 shows the interactions between the two microcontrollers on a time diagram captured by an oscilloscope. Three different types of communications are shown and the explanation of every step marked with number is described below.

1. The master MCU sends a command byte 0xAF, which orders the diagnostics MCU to measure all the channels of both ADCs.
2. The diagnostics MCU has received the command and initiates the ADC conversions by clearing both ADCs conversion start inputs for 2 µsec.
3. The ADCs put the end of conversion outputs low, indicating that the measurement results are ready in the FIFO. End of conversion signal goes high when the diagnostics MCU starts shifting data in from the ADC. SPI clock and data signals are not visible because they are on the second SPI bus of the diagnostics MCU.
4. When the diagnostics MCU has received the data from the ADCs and prepared the DMA, it puts the data ready output high for 2 µsec.
5. Since the data has to be transferred in only one direction, the main MCU starts transaction by sending a command byte 0xBF, followed by 29 bytes of zeros.

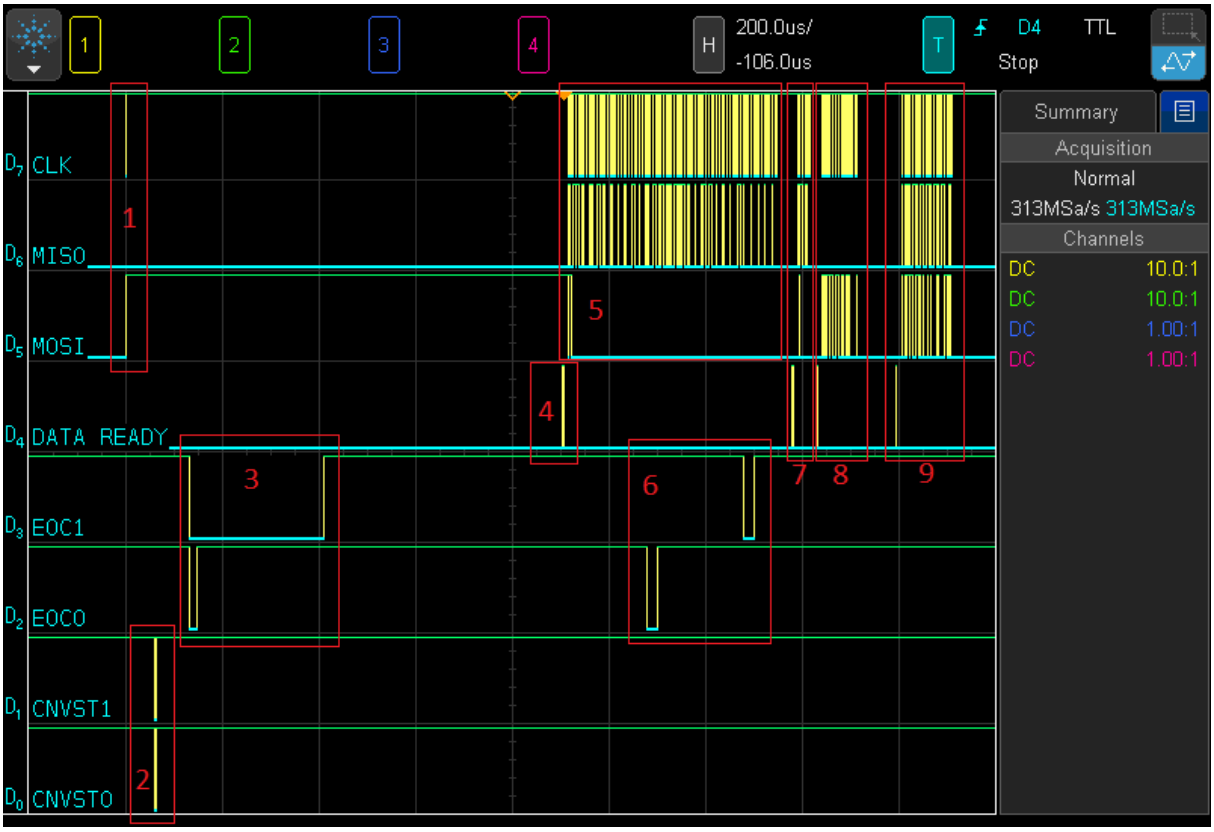

Figure 9: Oscilloscope screen capture taken during the execution of the example program.

6. During the data transfer with the main MCU, the diagnostics MCU starts processing the new command which instructs it to get the temperatures of both ADCs. EOC0 and EOC1 signals go low indicating the end of temperature conversions and go high when the MCU starts reading data from the ADC.
7. The diagnostics MCU sends data ready signal and the main MCU shifts the previously measured ADC temperatures in from the diagnostics MCU. This time the main MCU sends new command 0x22, meaning that the main MCU wants to send 10 bytes of data to the diagnostics MCU.
8. The diagnostics MCU acknowledges the request by sending data ready signal and the main MCU sends its data. A new command cannot be sent during the 10 byte transaction because the diagnostics MCU assumes that only data and no commands are being sent. The last spike in MOSI is 11^{th} byte containing a new command 0x11, meaning that the main MCU wants to swap 15 bytes of data.
9. The diagnostics MCU acknowledges the request and this time both MCUs send 15 bytes to each other.

5.6. Power consumption

The prototype´s power consumption was measured while both MCUs were doing their routine tasks including ADC measurements, data communication between the main and the diagnostics MCU, writing and reading from FRAM memory and sending data to UART. Table 1 describes the average current consumption of the main sections of the prototype.

The current measurements were conducted with a supply voltage of 3.301 V. The 10 mA current range was selected because it matched with theoretical maximums and it uses 1 Ω shunt resistor which minimizes the burden voltage [30]. 15000 current readings were collected during a time of one minute with the period of 4 milliseconds between each measurement.

Table 1: Power consumptions of the main sections of the prototype.

Device	Average current, µA	Teoretical current, µA
Diagnistics MCU	1394,1	1220[5]
Main MCU	1136,0	
2 x RS485 driver	796,9	900[6]
3 x FRAM	246,8	390[7]
ADC reference	130,8	150[8]
RTC	88,7	400[9]
Powerfail circuitry	17,3	13[10]
ADC0 + ADC1	7,3	3100[11]
Other peripherals	417,0	
Total	**4151,7**	

As the Table 1 states, the total current consumption is about 4.2 mA. This equals to 14 mW of power, which is an order of magnitude lower compared to ESTCube-1 EPS control electronics that was specified at 200 mW [12].

[5] 8 MHz clock, no FRAM wait-states, unified memory [23].
[6] In transmit mode [31].
[7] During data transaction at 1 MHz [32].
[8] In temperature range between −40°C to +125°C [29].
[9] During transaction with SPI clock 4 MHz, supply voltage 3.63 V, includes temperature measurement [14].
[10] With comparator input voltages: $V^+ = 2.7$ V and $V^- = 0$ V [26].
[11] Using external reference, during temperature measurement [27].

6. Summary

The aim of this thesis was to build a prototype of ESTCube-2 EPS subsystem control electronics. For that purpose, ESTCube-1 EPS was analyzed from the hardware perspective and all the areas where improvements could be made were listed. The requirements for ESTCube-2 EPS control electronics were set and a new design was implemented that improves the functionality and the reliability of the system while making it more robust. The testing results showed that the prototype meets or exceeds all the requirements that were set. The main results are following:

- the supply voltage of the system is 3.3 V;
- power consumption of 14 mW was achieved which is less than the requested maximum of 30 mW;
- the prototype has 30 external ADC input channels which are measured within a time window of 70 µsec. The number of the ADCs can be incremented with no increase in the acquisition time;
- the system includes voltage fault detection system that notifies the MCU about the voltage fault and holds the system operational for about 200 milliseconds.

The hardware module that was built during the practical work has two separate microcontroller units - one for general tasks and other for diagnostics purpose. The prototype features 3.3 V voltage regulator for obtaining supply from the USB port, pin headers between the main supply and individual sections supply lines as well as in the inputs and outputs of all peripheral devices, debugging LEDs and test points for convenient debugging. The module can be easily connected to other EPS subsystem´s prototypes.

The low level software that was written utilizes direct memory access that allows high speed data connection between two microcontrollers. The software is written in C language and enables to reuse the high level software of the ESTCube-1 thanks to similar function arguments and return types.

ESTCube-2 elektrienergia alamsüsteemi juhtelektroonika prototüübi ehitamine ning testimine

Martin Põder

7. Kokkuvõte

ESTCube-2 ja ESTCube-3 on Eesti tudengisatelliidi projekti jätkumissioonidena kavandatavad satelliidid. Nende peamine eemärk on testida elektrilist päikesetuulepurjet suuremal skaalal ning väljaspool planeet Maa magnetvälja, näiteks Kuu orbiidil. ESTCube-2 missioon seisneb elektrilise päikesetuulepurje komponentide ja teiste ESTCube-3 kasutatavate alamsüsteemide testimises maalähedasel orbiidil. Kuna ESTCube-2 on suurema energiavajadusega kui Eesti esimene satelliit ESTCube-1, tuleb selle rahuldamiseks disainida uus elektrienergia alamsüsteem.

Käesolev bakalaureusetöö analüüsib ESTCube-1 elektrienergia alamsüsteemi riistvara seisukohalt, pakub välja lahendused ilmnenud kitsaskohtade parandamiseks, püstitab ESTCube-2 elektrienergia alamsüsteemi juhtelektroonika funktsionaalsed nõuded ning kirjeldab prototüübi valmimist ja testimise tulemusi.

Praktilise töö tulemusena valmis prototüüp, mis parandas ESTCube-1 elektrienergia alamsüsteemi kontrollelektroonikal ilmnenud kitsaskohad. Samuti täitis või ületas prototüüp kõiki sellele esitatud nõuded. Töö tulemusena valminud prototüübi olulisemad omadused on:

- 3.3 voldine toitepinge;
- seadme energiatarve 14 mW, mis on kaks korda vähem püstitatud maksimaalsest väärtusest (30 mW);
- 30 analoog-digitaalmuundi sisendit, mille mõõtetulemused saadakse 70 mikrosekundiga. Analoog-digitaalmuundite arvu saab skeemis suurendada selliselt, et mõõteaeg sellest ei pikene;
- toitepinge kadumist tuvastav ahel, mis teatab mikrokontrollerit pinge kadumisest ning mille mahtuvuspank hoiab süsteemi töös 200 millisekundit pärast vea ilmnemist.

Valminud prototüübil on kaks mikrokontrollerit, millest üks tegeleb ainult diagnostikaga ning teine kõigi ülejäänud ülesannetega. Prototüübil on 3.3 V pingeregulaator, et toita seda USB pordist, väljaviigud kõikide alamosade sisendites, väljundites ning toitepinge ahelates. Samuti on trükkplaadile lisatud hulganisti mõõteväljaviike ning valgusdioode, mis lihtsustavad vea otsingut ja silumist. Prototüüpi on lihtne kasutada ja täiendada teiste elektrienergia alamsüsteemi osadega ühtseks tervikuks.

Prototüübi jaoks arendatud tarkvara kasutab otsemälupöördust, et tagada kiire andmevahetus kahe mikrokontrolleri vahel. Tarkvara on kirjutatud C keeles ning võimaldab taaskasutada ESTCube-1 kõrgema taseme tarkvara, sest funktsioonide argumendid ja tagastustüübid on sarnased ESTCube-1 tarkvaraga.

References

[1] ESTCube, “Estonia student satellite programme,” 2013. [Online]. Available: http://www.estcube.eu/. [Accessed 15 April 2015].

[2] P. Janhunen, “Electric sail for spacecraft propulsion,” *AIAA Journal of Propulsion and Power,* vol. 4, no. 20, pp. 763-764, 2004.

[3] E. Ilbis, M. Pajusalu, T. Ilves, R. Raabe, M. Veske, G. Olentšenko, E. Briede, S. Lätt and M. Noorma, “Electrical power system for ESTCube-1 nanosatellite: lessons learned from in-orbit operations,” Tartu, 2015. Unpublished.

[4] California Polytechnic State University, “CubeSat Design Specification revision 13,” 2014.

[5] J. Envall, P. Janhunen, P. Toivanen, M. Pajusalu, E. Ilbis, J. Kalde, M. Averin, H. Kuuste, K. Laizans, V. Allik, T. Rauhala, H. Seppänen, S. Kiprich, E. Haeggström, T. Kalvas, O. Tarvainen, J. Kauppinen, A. Nuottajärvi and H. Koivisto, “E-sail test payload of the ESTCube-1 nanosatellite,” *Proceedings of the Estonian Academy of Sciences,* vol. 2S, no. 63, pp. 210-221, 2014.

[6] K. O. Skyttemyr, “Design and Implementation of the Electrical Power System for the CubeSTAR Satellite,” master´s thesis 2013.

[7] Aalborg University, “AAUSAT3 in details,” 2013. [Online]. Available: http://www.space.aau.dk/aausat3/index.php?n=Tech.Eps. [Accessed 19 May 2015].

[8] P. Thirion, „Design and Implementation of On-board Electrical Power Supply of Student NanosatelliteOUFTI-1 of University of Liège,“ master´s thesis 2009.

[9] L. E. Jacobsen, „Electrical Power System of the NTNU Test Satellite,“ 2011.

[10] Atmel, „ATmega640/V-1280/V-1281/V-2560/V-2561/V,“ 2014.

[11] K. Avery, J. Fenchel, J. Mee, W. Kemp, R. Netzer, D. Elkins, B. Zufelt and D. Alexander, “Total Dose Test Results for CubeSat Electronics,” Radiation Effects Data Workshop, Las Vegas, 2011.

[12] E. Ilbis, „ESTCube-1 Electrical Power System - design, implementation and testing,“ bachelor´s thesis 2013.

[13] Maxim Integrated, “MAX6369-MAX6374 Pin-Selectable Watchdog Timers,” 2011.

[14] Maxim Integrated, “DS3234 Extremely Accurate SPI Bus RTC with Integrated Crystal and SRAM,” 2015.

[15] “SPI Bus interface,” 2006. [Online]. Available: http://www.eeherald.com/section/design-guide/esmod12.html. [Accessed 18 April 2015].

[16] Texas Instruments, “MSP430™ Programming Via the JTAG Interface,” 2015.

[17] Texas Instruments, “MSP-EXP430FR5969 LaunchPad™ Development Kit,” 2014.

[18] C. Sansoè and M. Tranchero, “Use of FRAM Memories in Spacecrafts,” Italy, 2011.

[19] Texas Instruments, “MSP430FR698x, MSP430FR598x Mixed-Signal Microcontrollers,” 2015.

[20] Advanticsys, “Product CM5000,” 2015. [Online]. Available: http://www.advanticsys.com/shop/mtmcm5000msp-p-14.html. [Accessed 18 April 2015].

[21] T. Vladimirova, C. P. Bridges, G. Prassinos, X. Wu, K. Sidibeh, D. J. Barnhart, A.-H. Jallad, J. R. Paul, V. Lappas, A. Baker, K. Maynard and R. Magness, “Characterising Wireless Sensor Motes for Space Applications,” in *Second NASA/ESA Conference on Adaptive Hardware and Systems*, Edinburgh, 2007.

[22] J. Kalde, “Piezoelectric motor driver for CubeSat,” bachelor´s thesis 2013.

[23] Texas Instuments, “MSP430FR59xx Mixed-Signal Microcontrollers,” 2015.

[24] Texas Instruments, “MSP430FR58xx, MSP430FR59xx, MSP430FR68xx, and MSP430FR69xx Family User's Guide,” 2015.

[25] Linear Technology, “LTC4412 Low Loss PowerPath™ Controller in ThinSOT,” 2002.

[26] Texas Instruments, “Single & Dual, 1.8V Low Power Comparators with Rail-to-Rail input,” 2013.

[27] Maxim Integrated, “12-Bit 300ksps ADCs with FIFO, Temp Sensor, Internal Reference,” 2012.

[28] Maxim Integrated, “12-Bit, Multichannel ADCs/DACs with FIFO, Temperature Sensing and GPIO Ports,” 2015.

[29] Analog Devices, “Low Power, Low Noise Voltage References with Sink/Source Capability,” 2010.

[30] Tektronix, “Digital Multimeters Tektronix DMM4050 and DMM4040,” 2013.

[31] Linear Technology, “3.3V 20Mbps RS485/RS422 Transceivers,” 2007.

[32] Cypress, “FM25V20 2-Mbit (256 K × 8) Serial (SPI) F-RAM,” 2014.

Appendices

Appendix 1 - Schematics

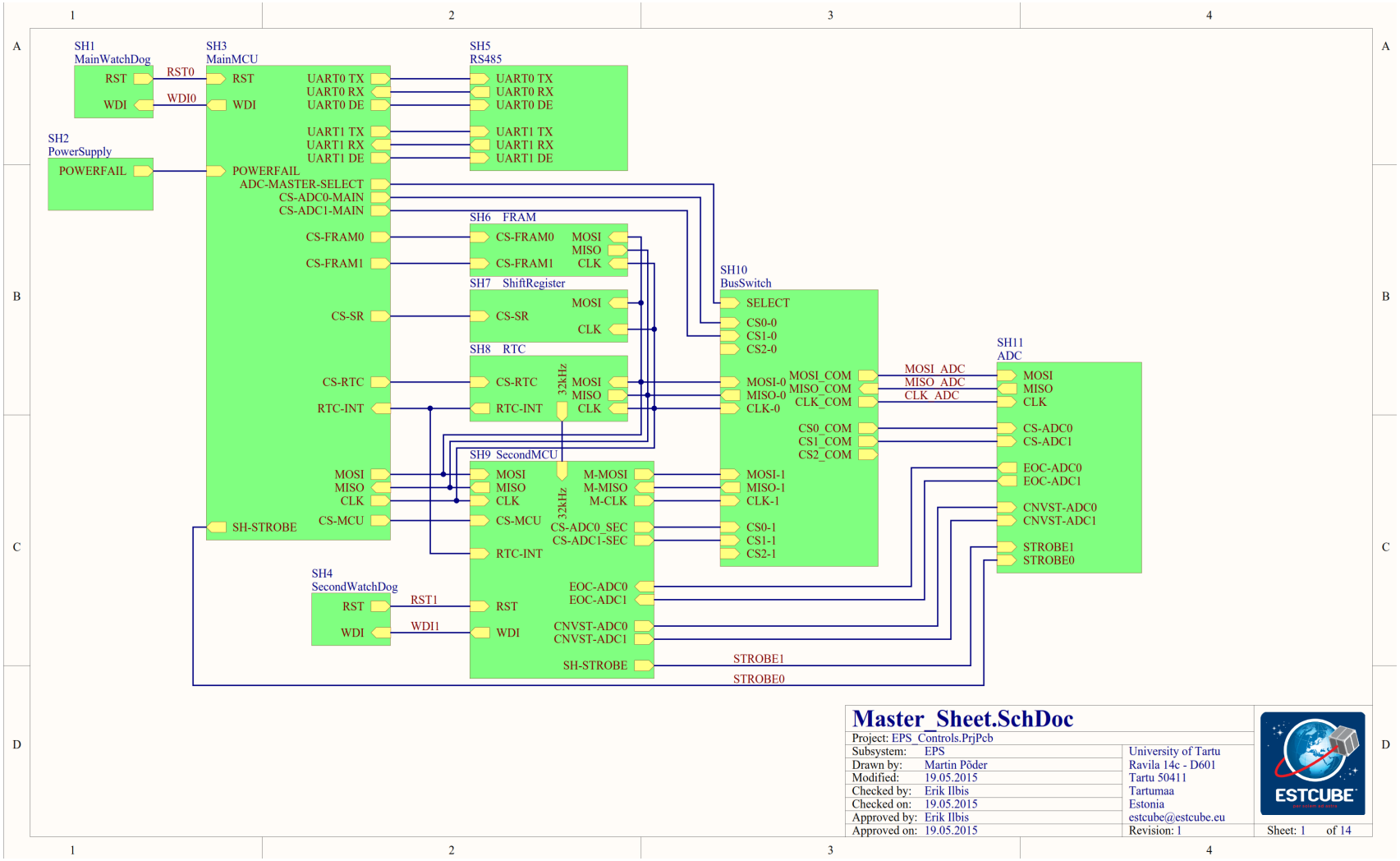

Figure 10: The main sheet of schematics.

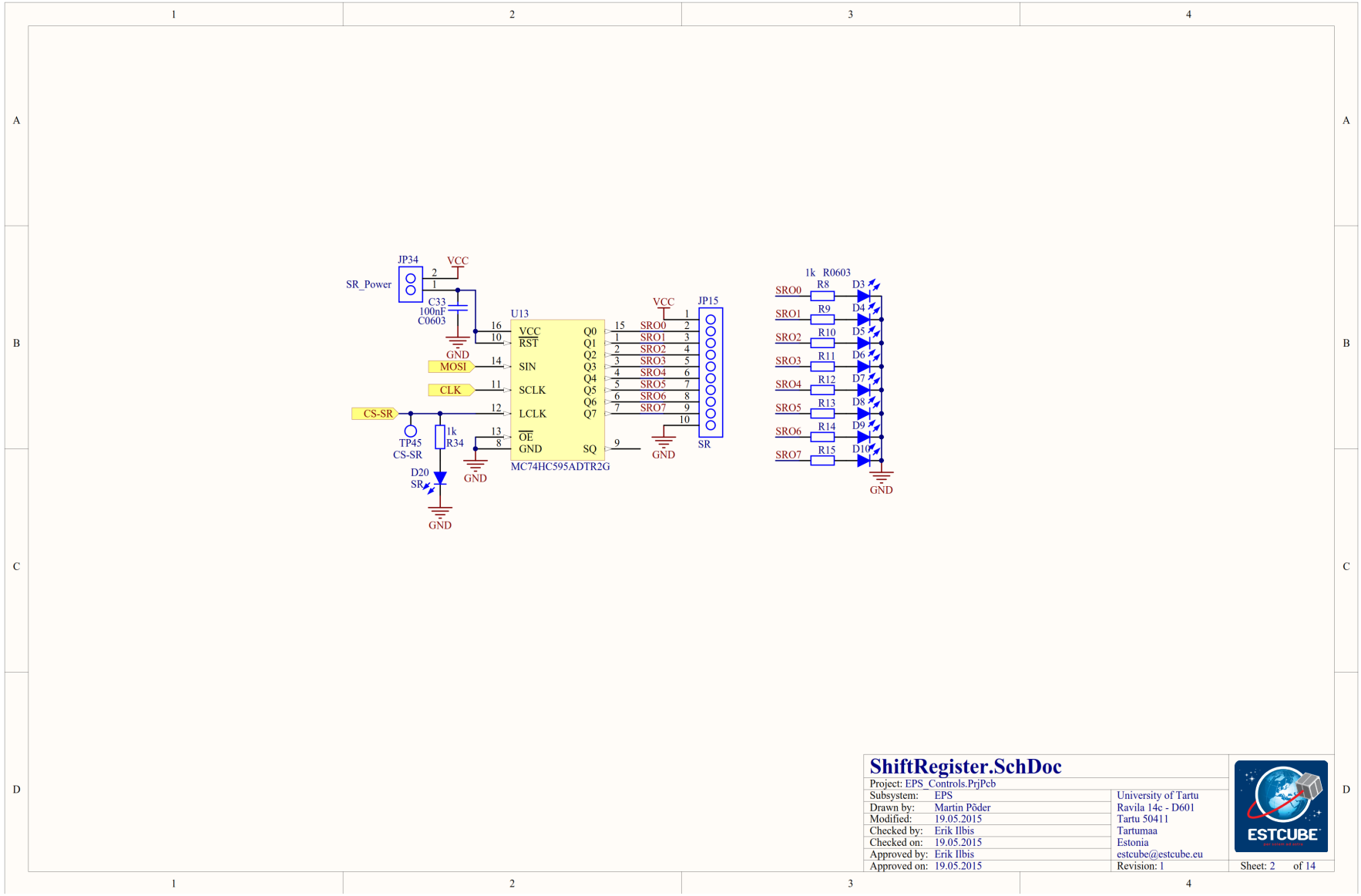

Figure 11: Shift register.

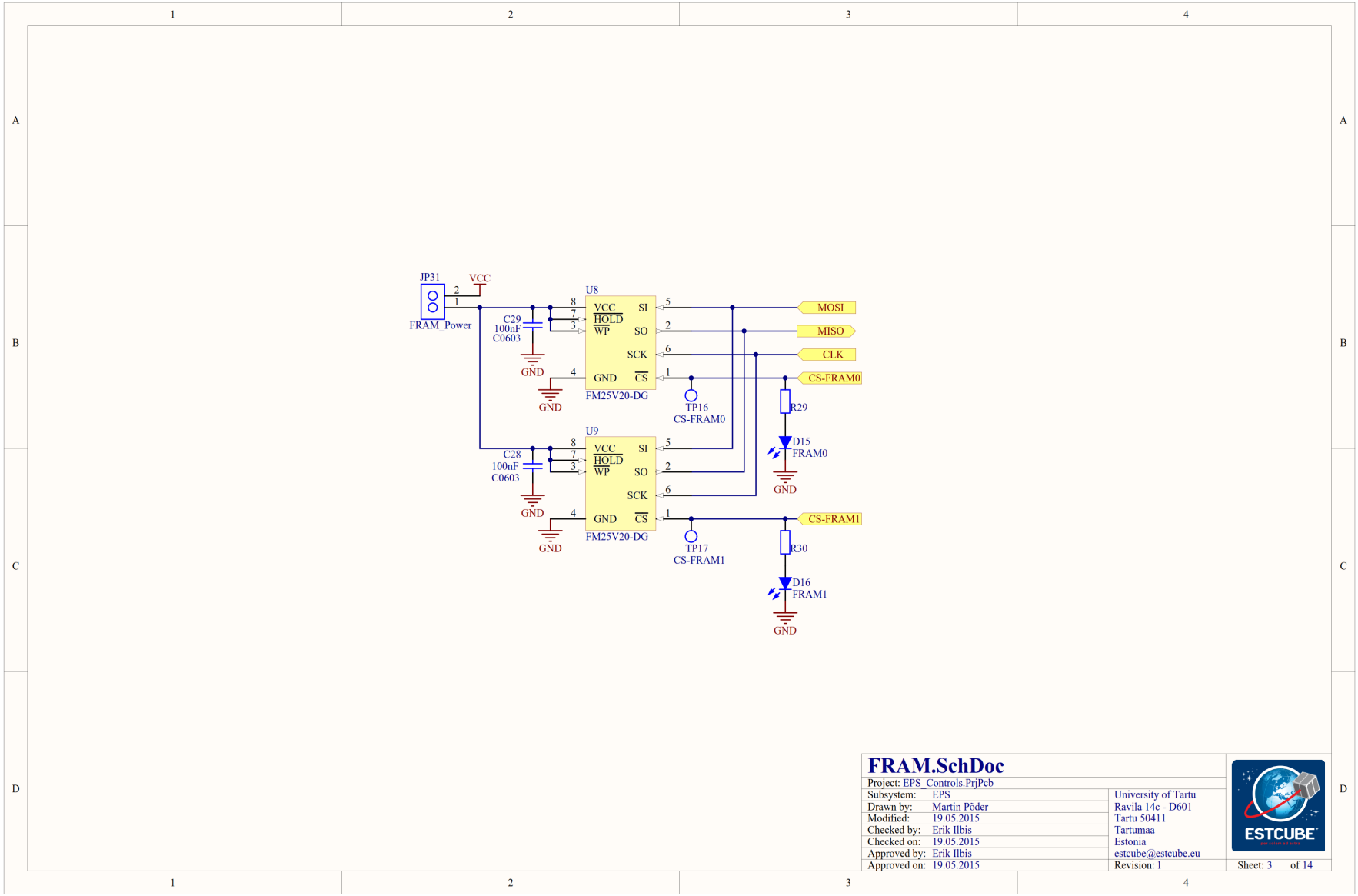

Figure 12: FRAM memories.

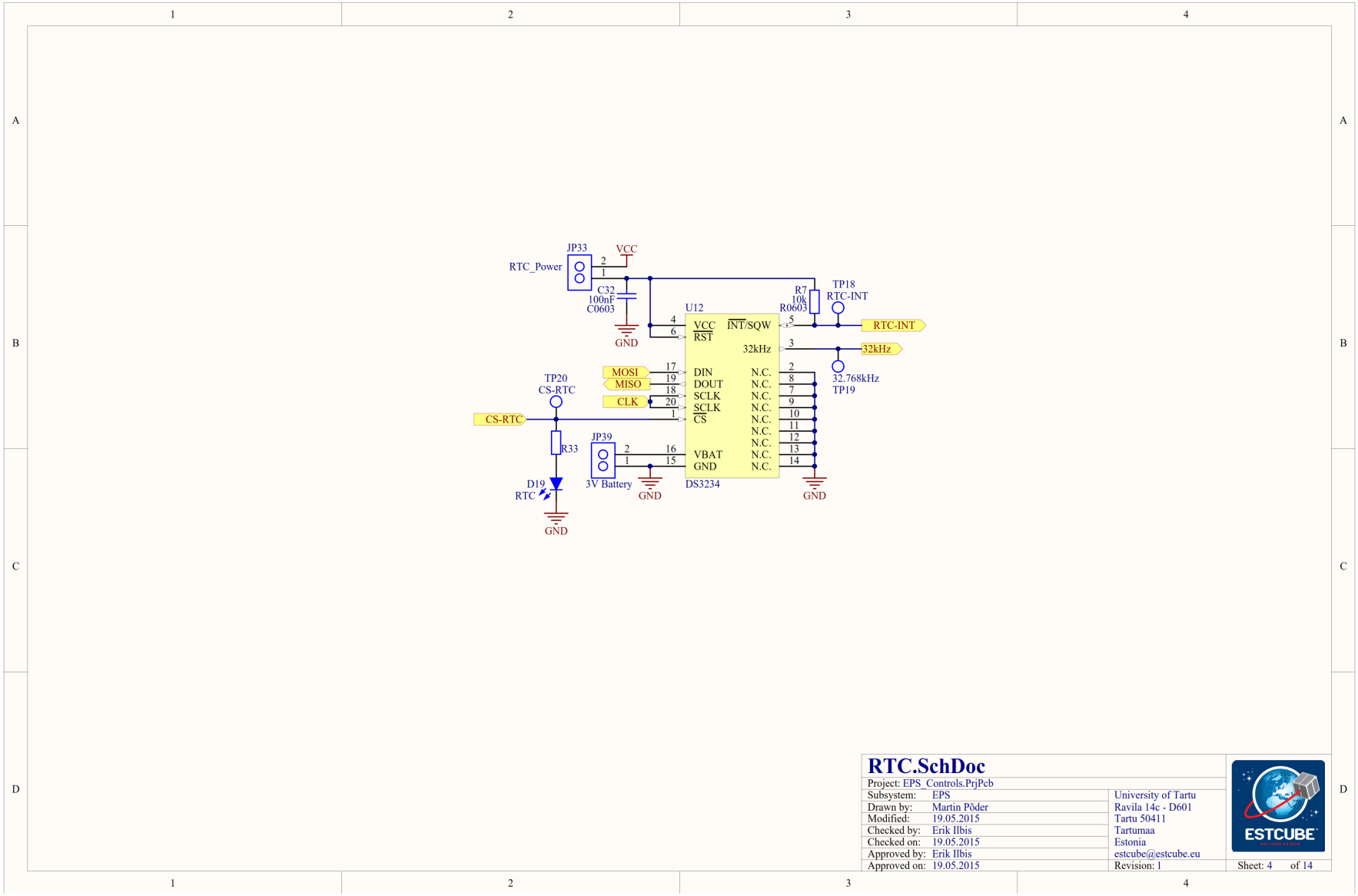

Figure 13: Real-time clock.

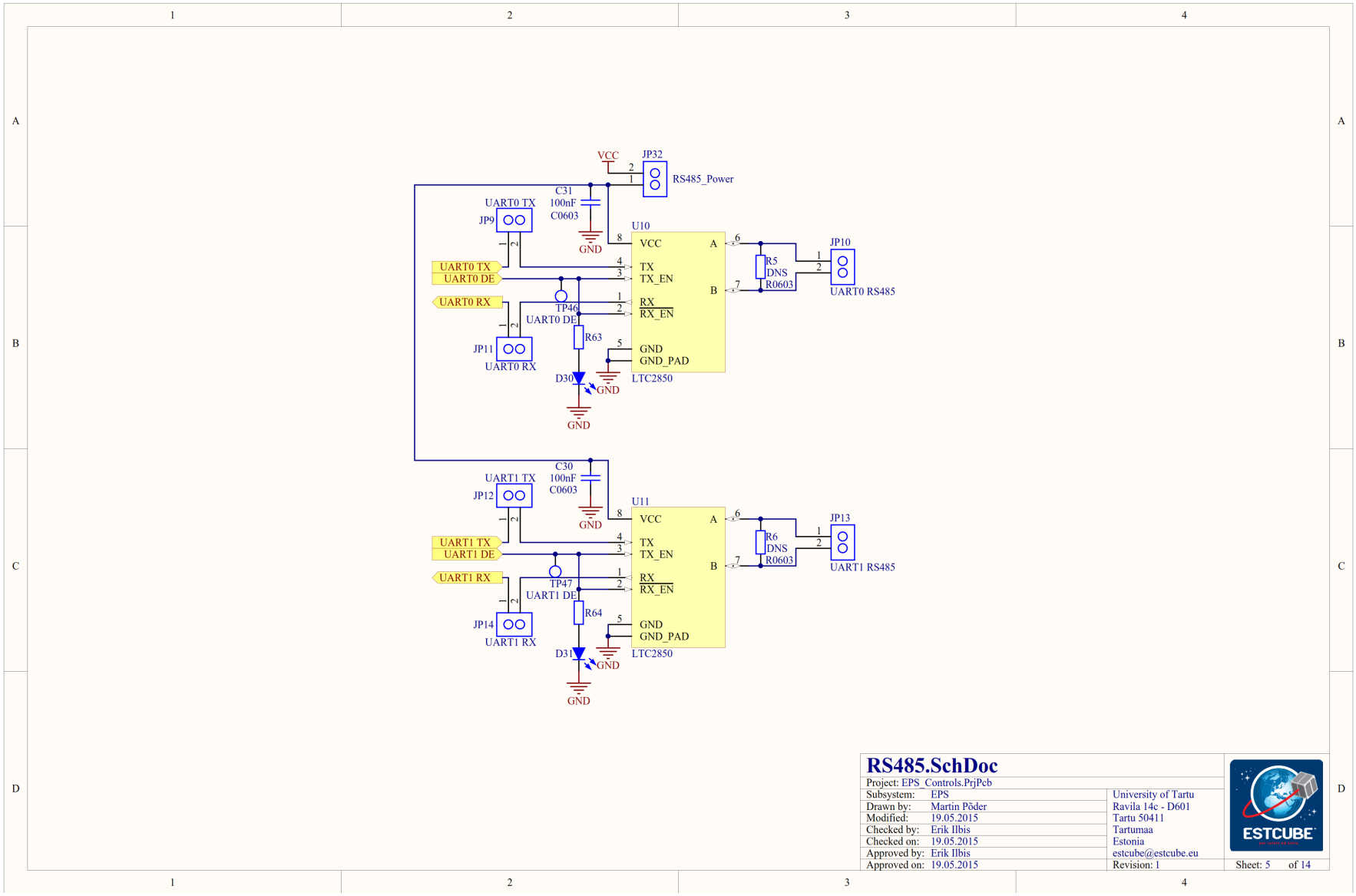

Figure 14: RS485 transceivers.

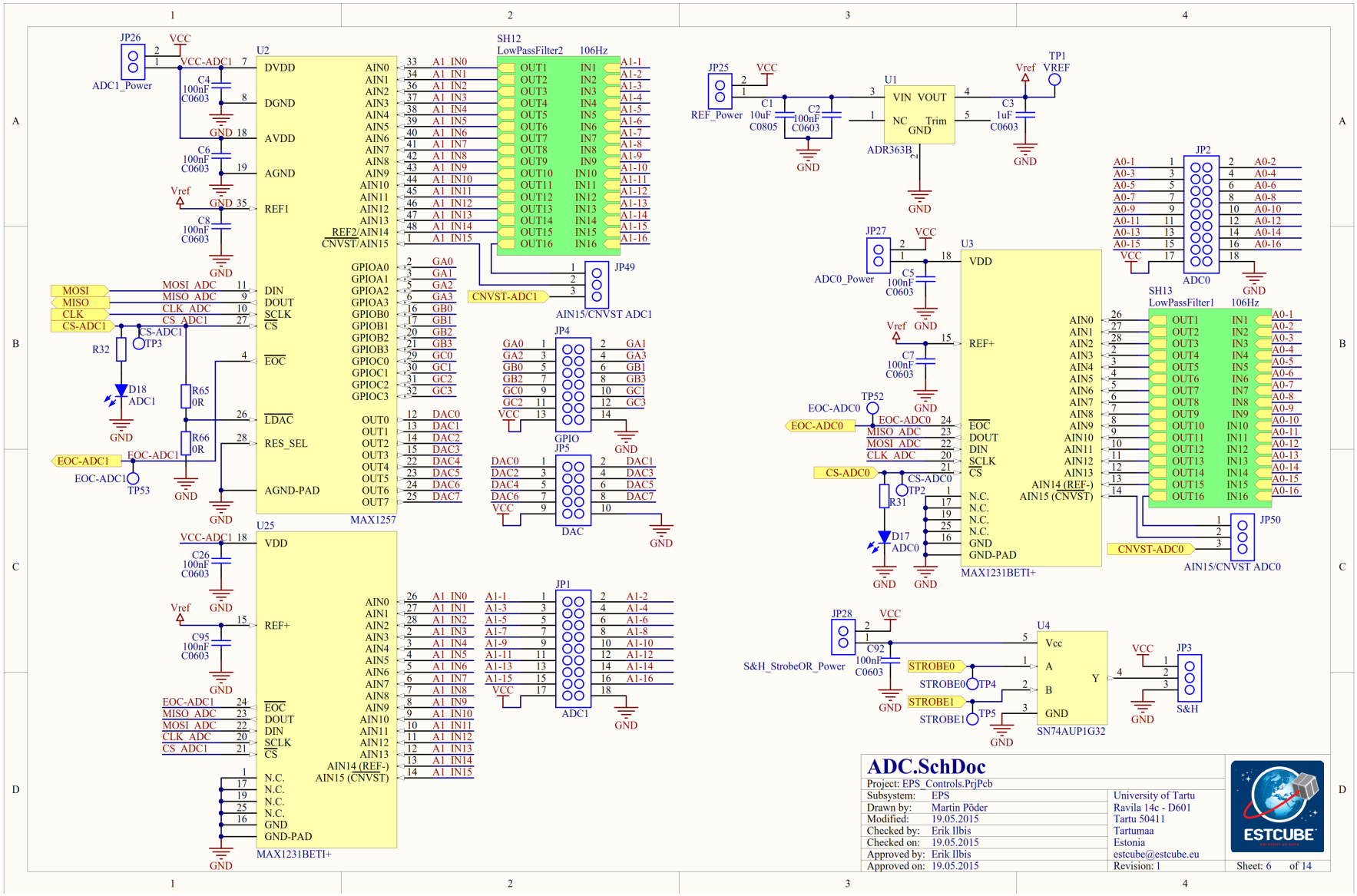

Figure 15: Analog-to-digital converters.

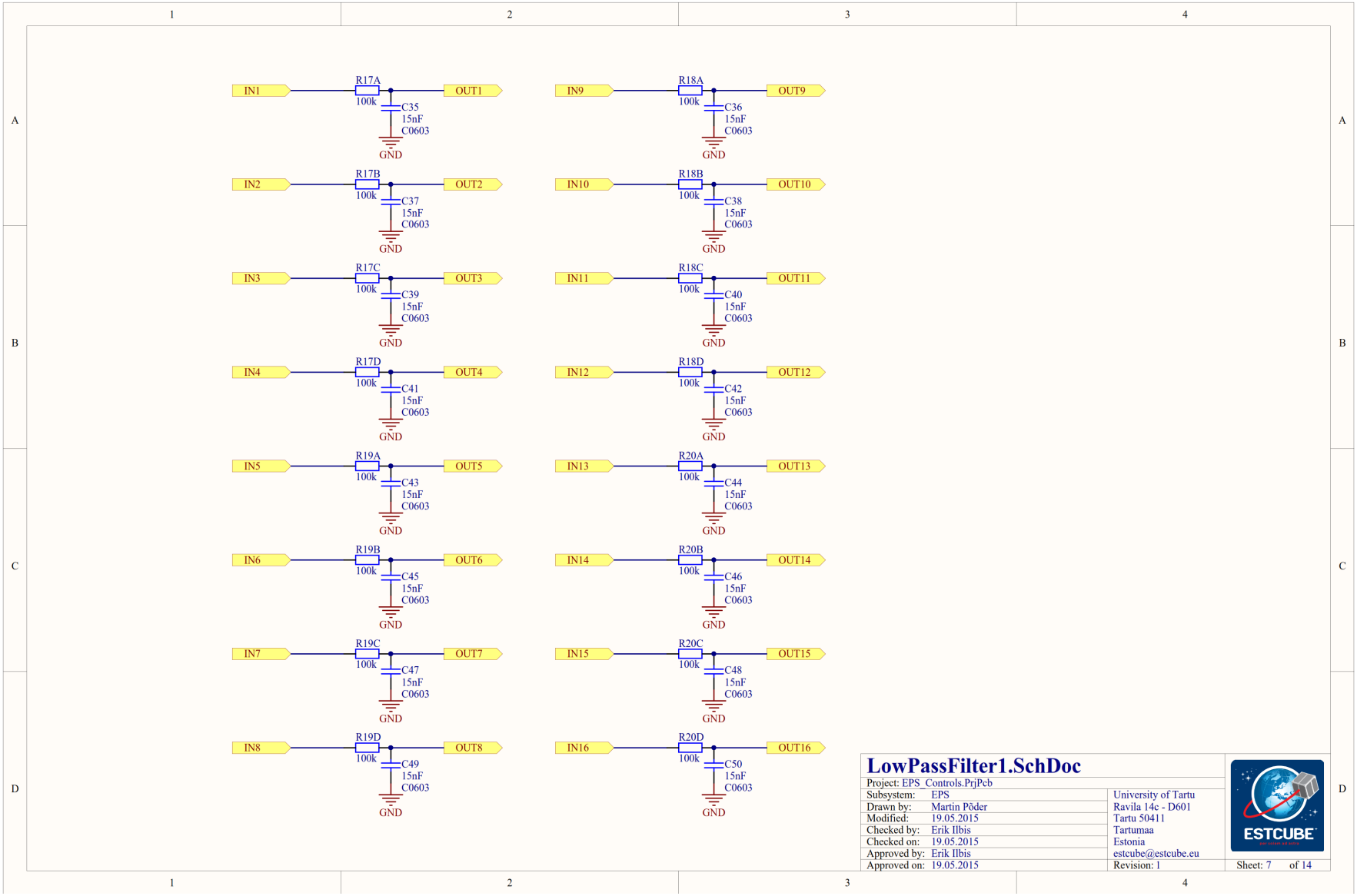

Figure 16: Low pass filter of ADC0.

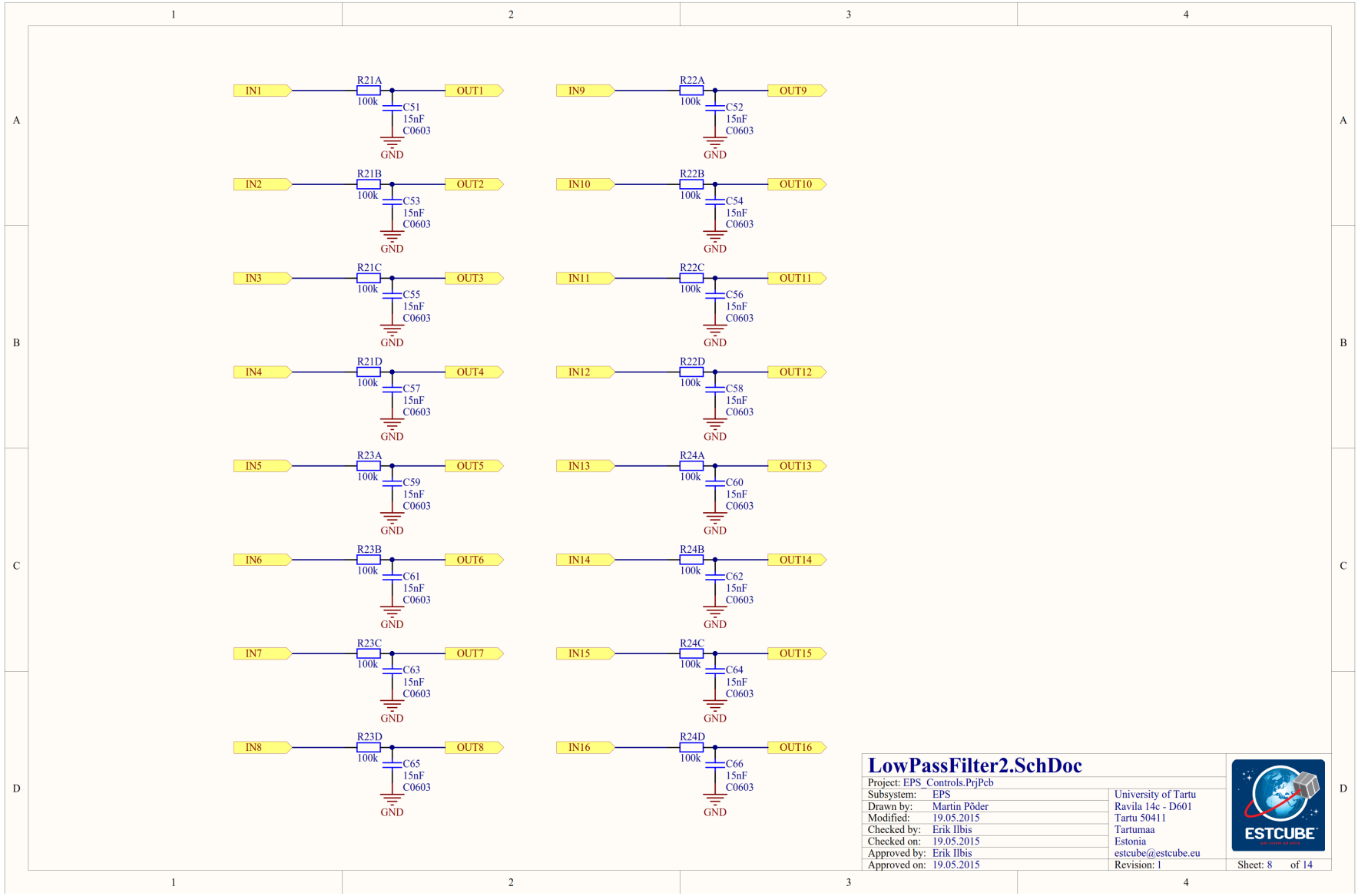

Figure 17: Low pass filter of ADC1.

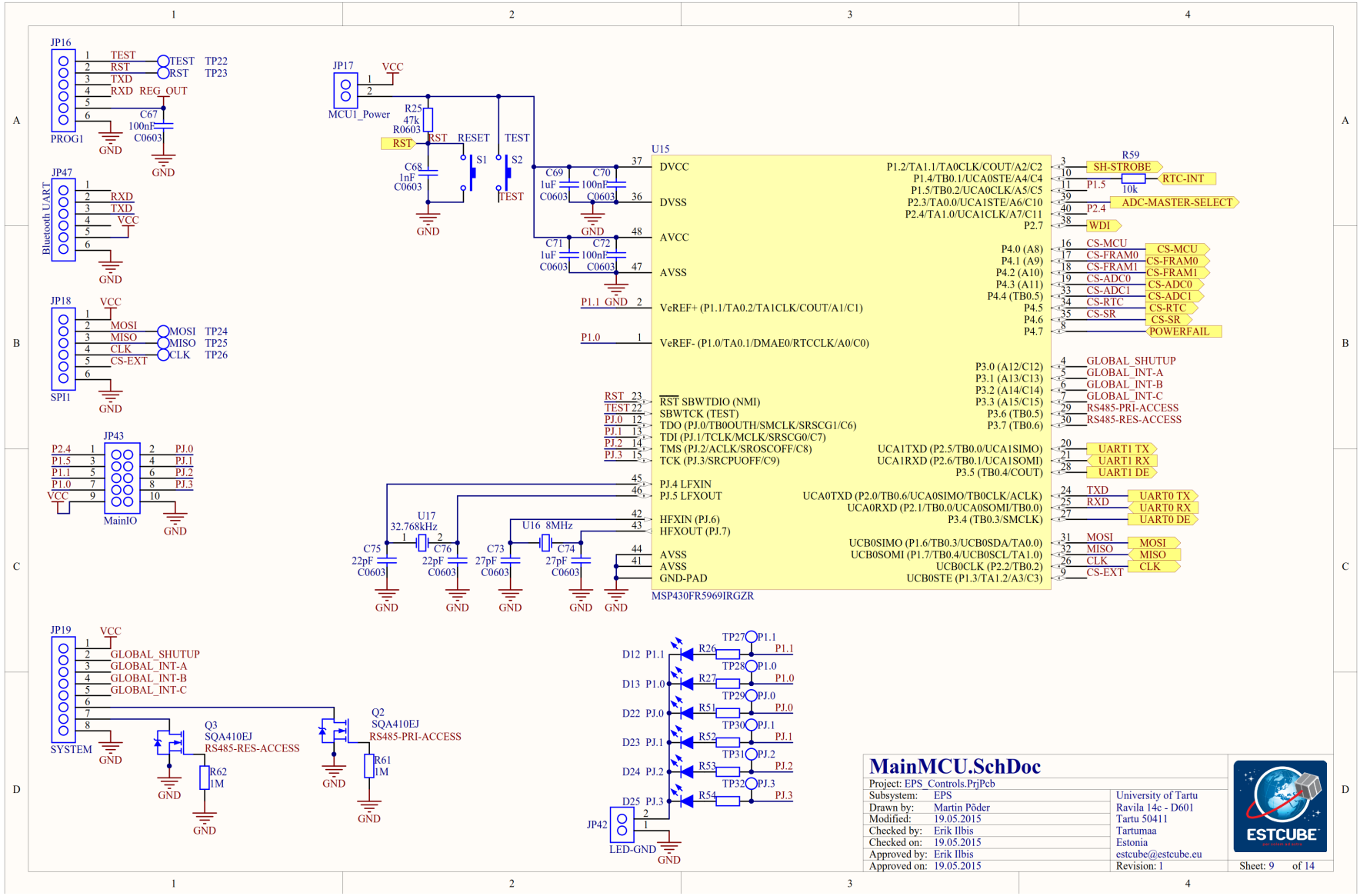

Figure 18: Main microcontroller unit.

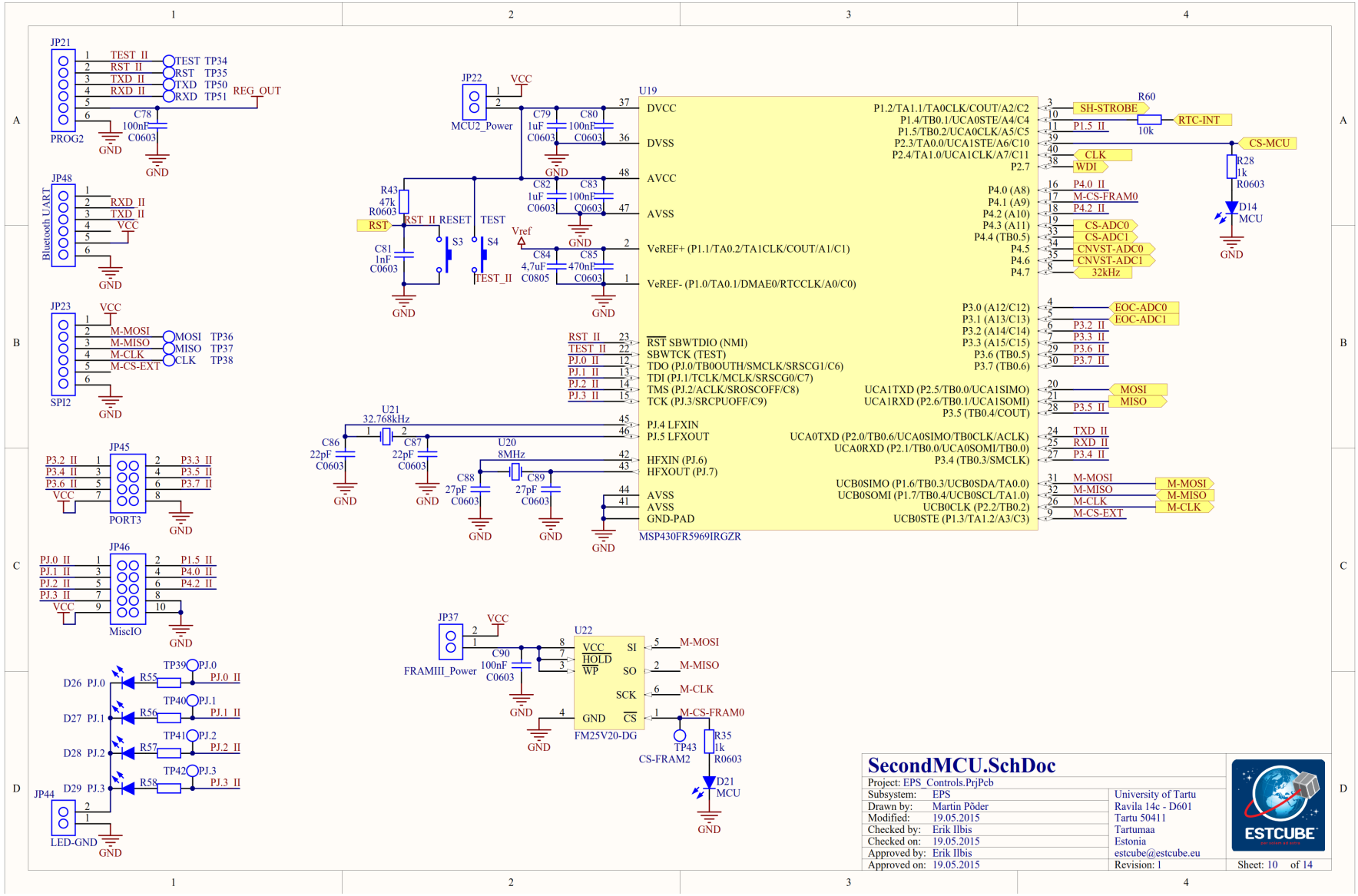

Figure 19: Second microcontroller unit.

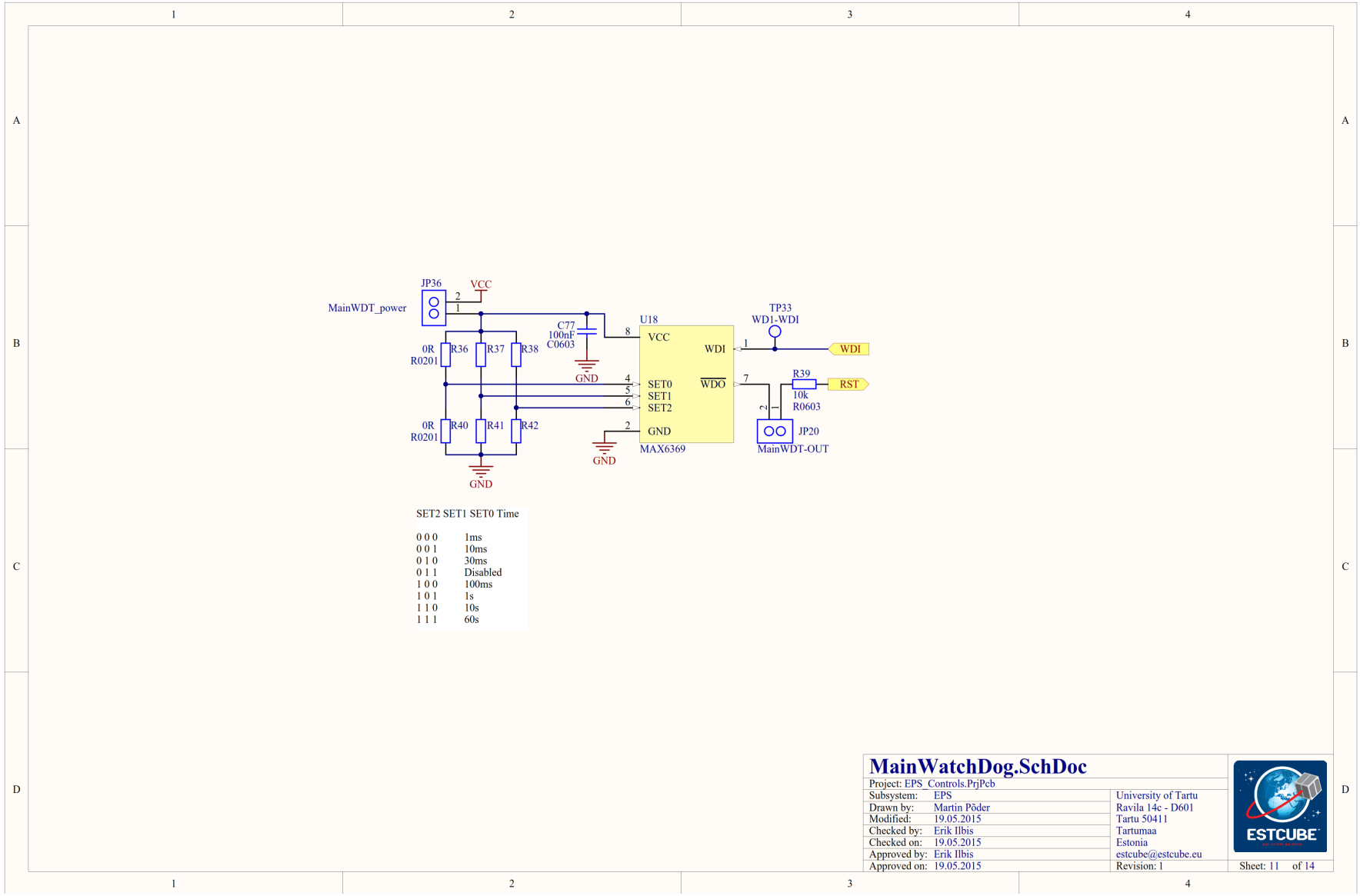

Figure 20: External watchdog timer of the main MCU.

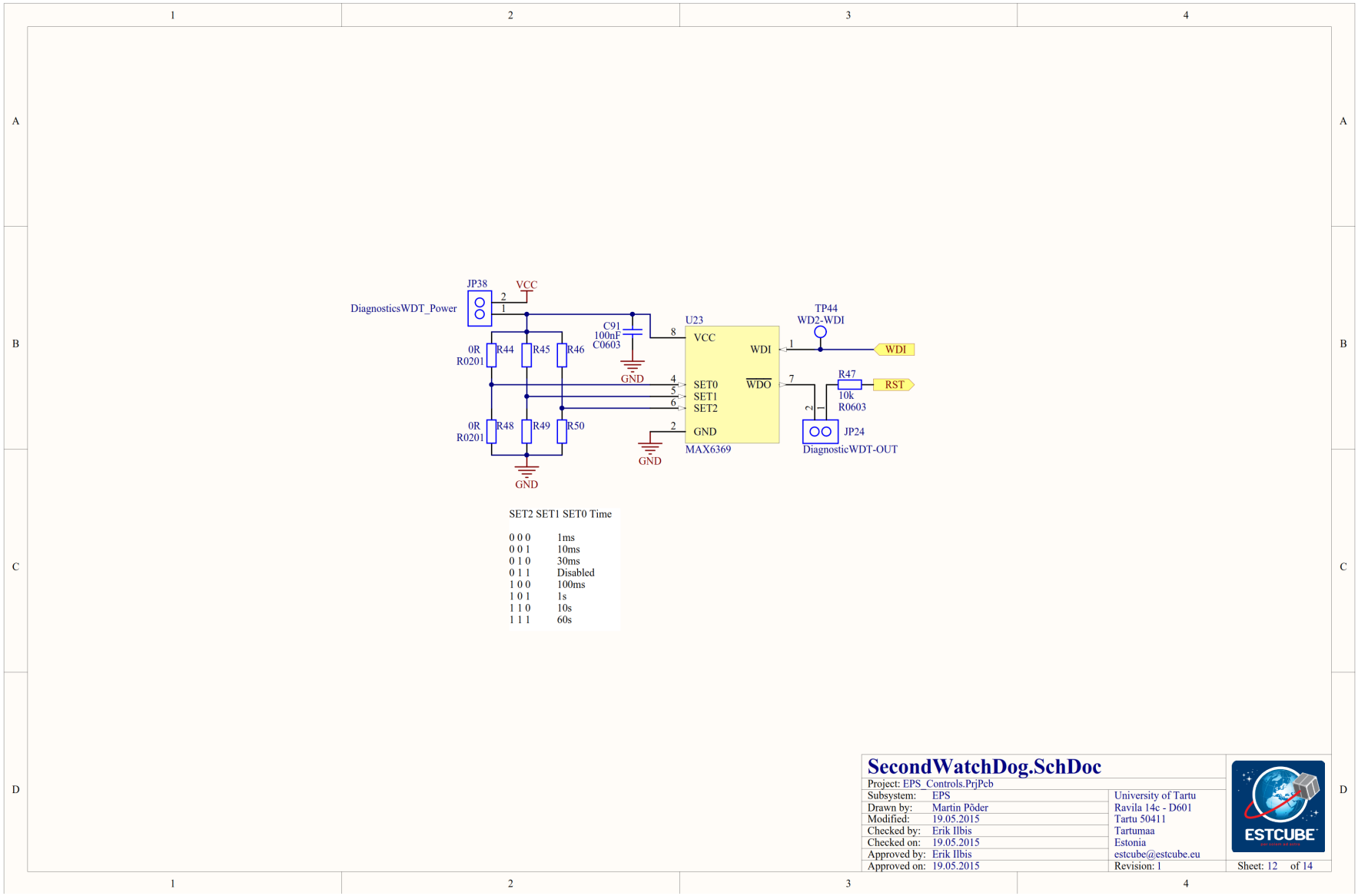

Figure 21: External watchdog timer of second MCU.

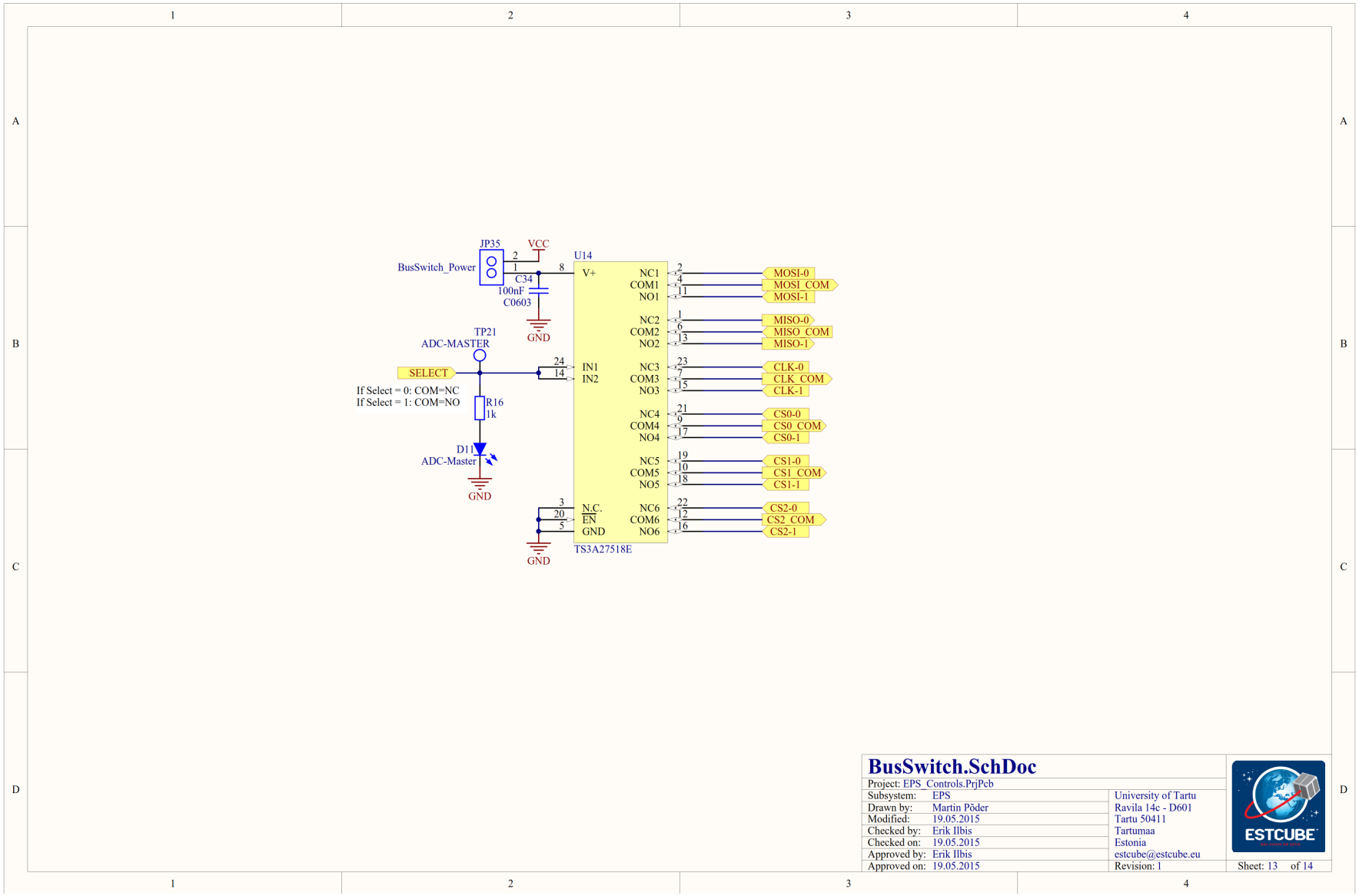

Figure 22: Bus switch.

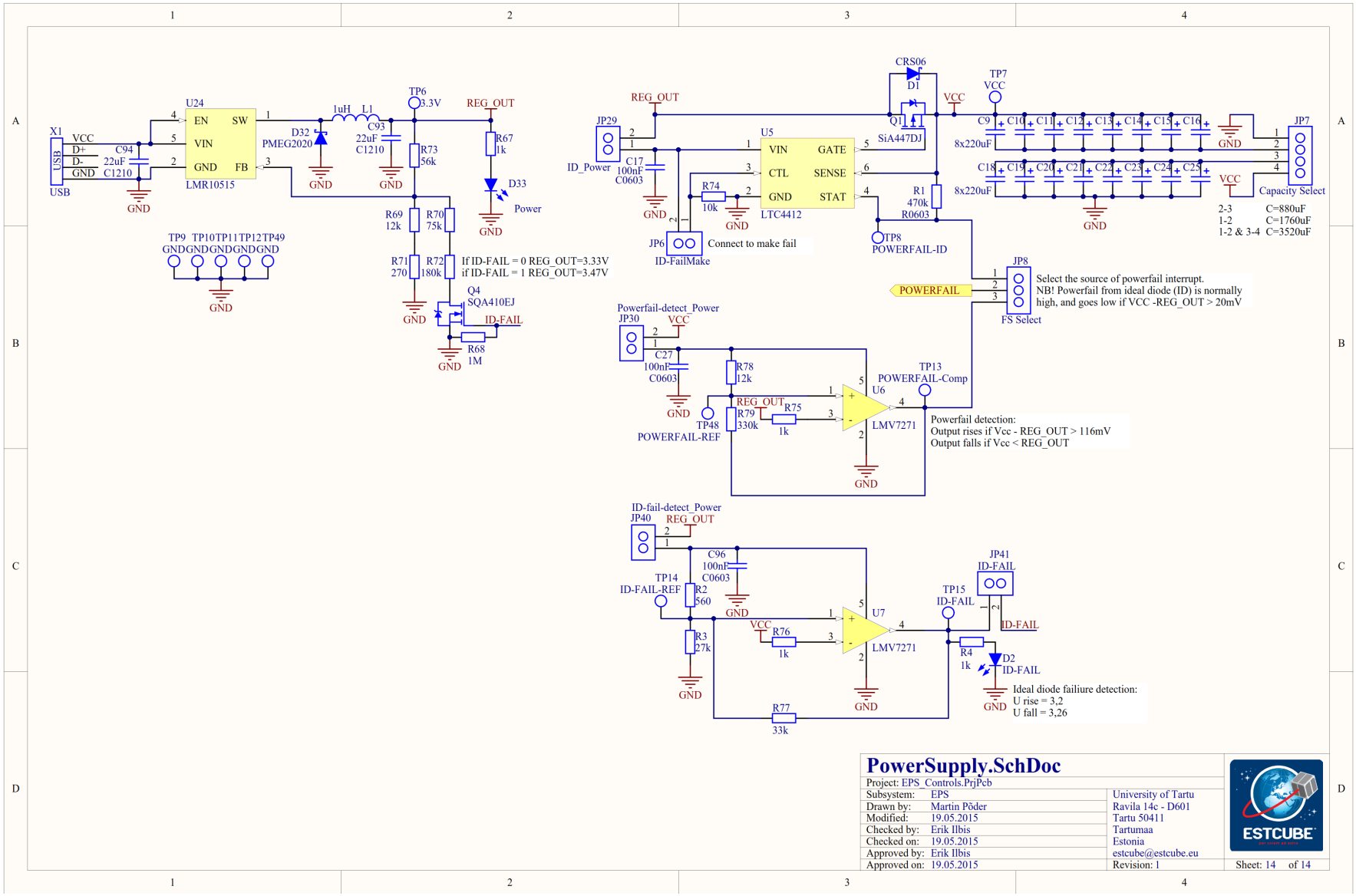

Figure 23: Power supply with capacitor bank and powerfail detection circuitry.

Appendix 2 - PCB design

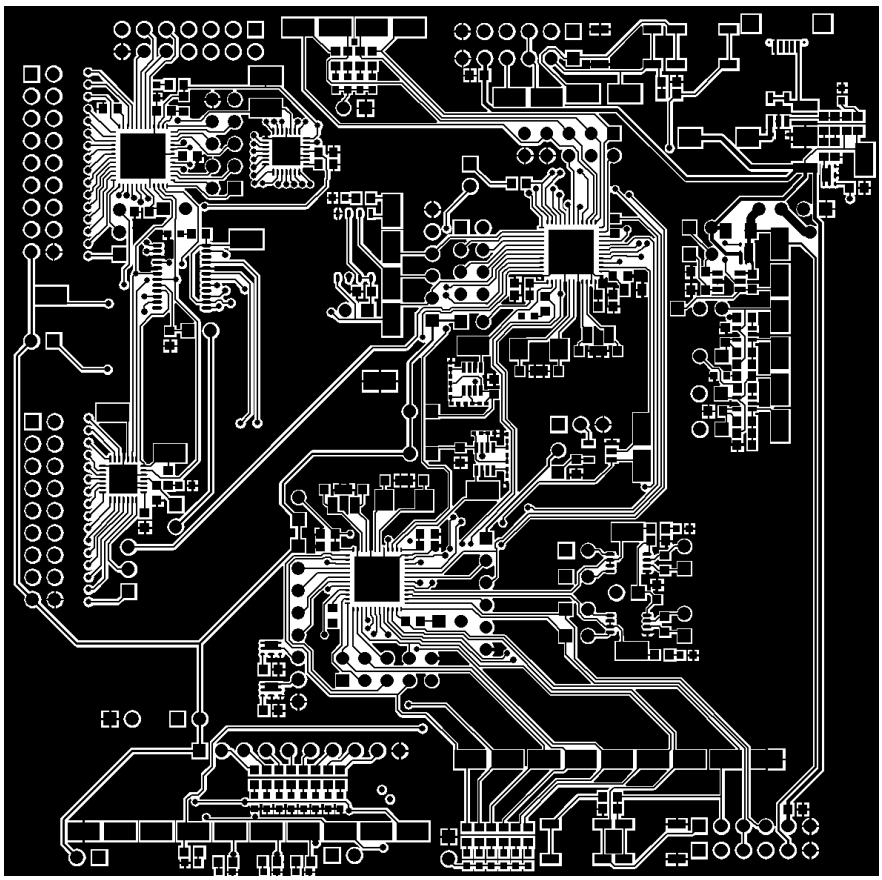

Figure 24: Top copper layer.

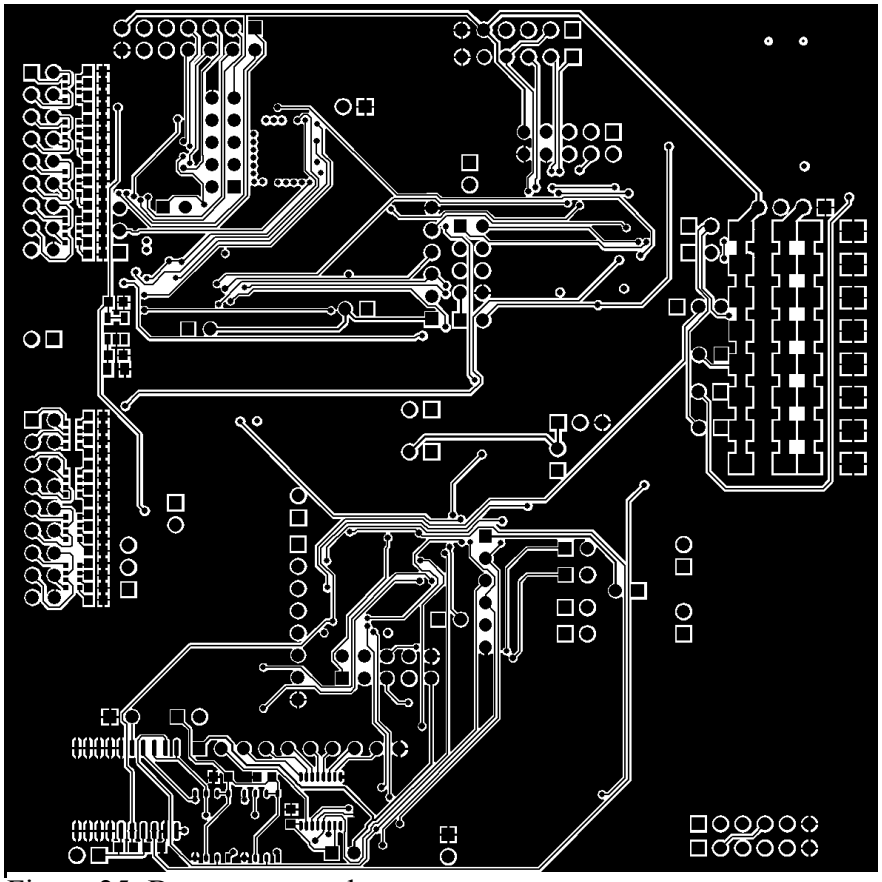

Figure 25: Bottom copper layer.

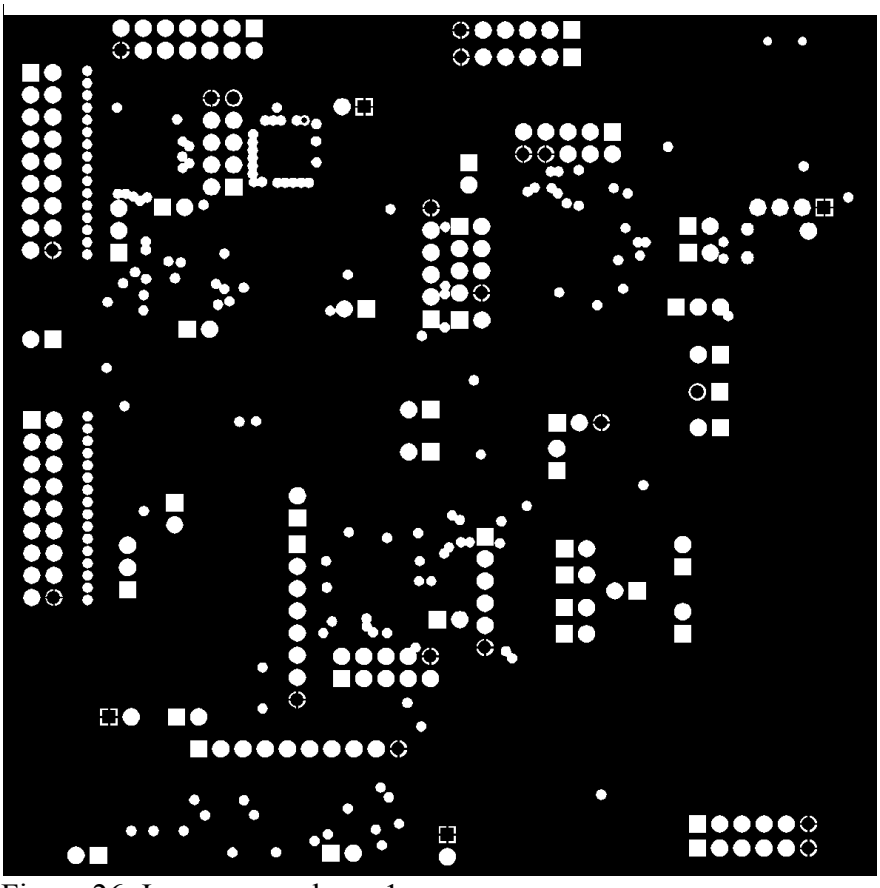

Figure 26: Inner copper layer 1.

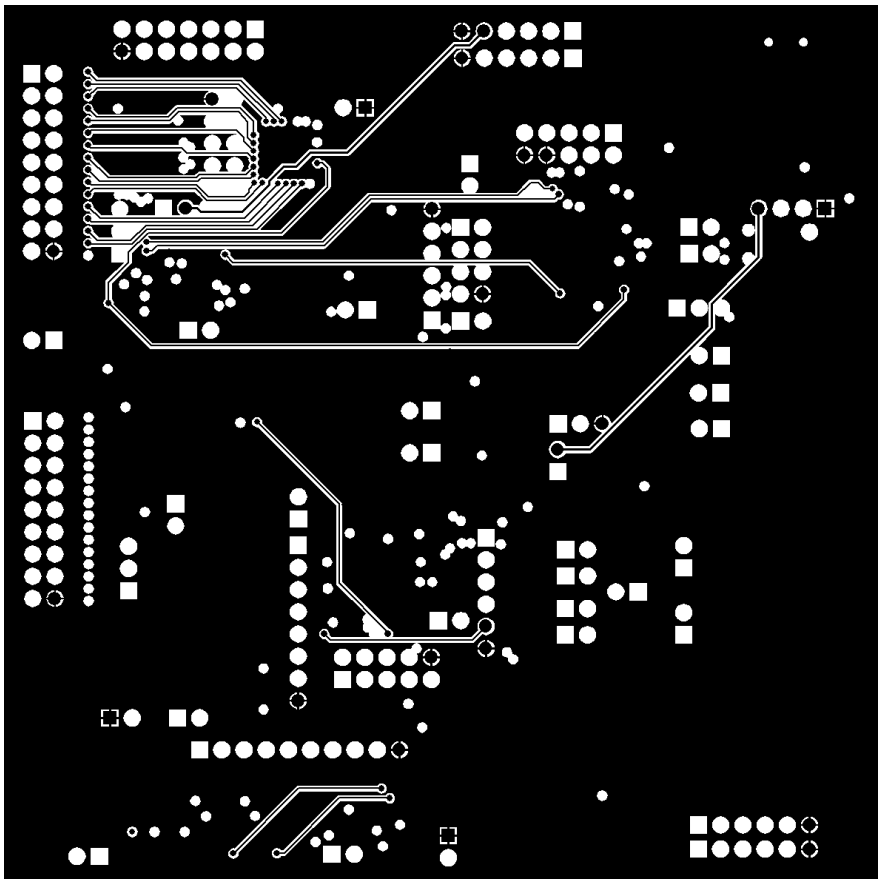

Figure 27: Inner copper layer 2.

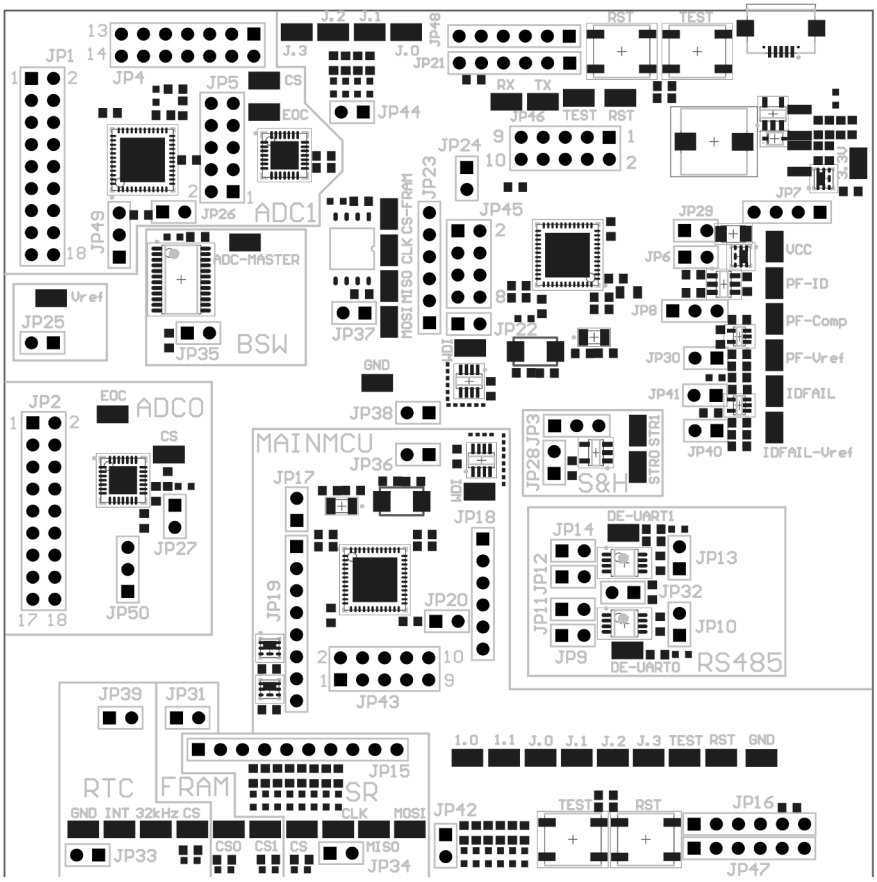

Figure 28: Top assembly and silkscreen layers.

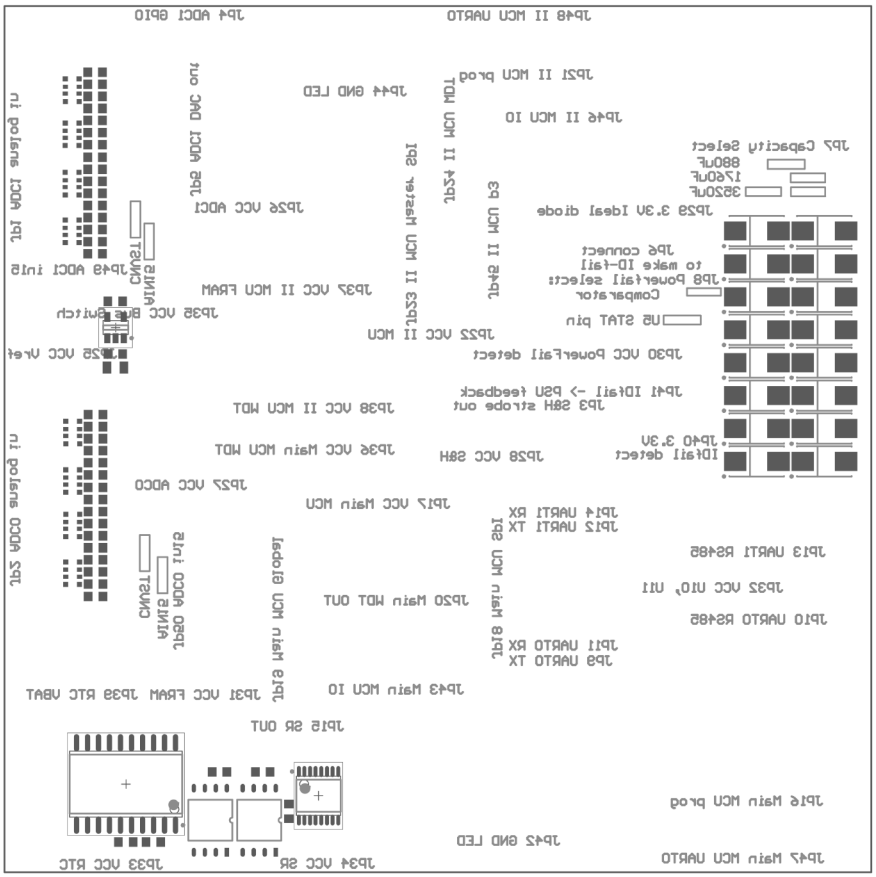

Figure 29: Bottom assembly and silkscreen layers.

Acknowledgements

I would like to thank my supervisors Mihkel Pajusalu and especially Erik Ilbis, who gave me this challenging thesis topic, supported me with his knowledge and gave me lots of practical guidance during the prototype design.

I would also like to thank the Protokeskus of the University of Tartu for allowing me to use their electronics lab for soldering and testing the prototype, and the entire ESTCube team for giving the opportunity to build a satellite. It was my utmost honour to participate in the development of ESTCube-2.

Non-exclusive licence to reproduce thesis and make thesis public

I, Martin Põder, herewith grant the University of Tartu a free permit (non-exclusive licence) to:

1.1. reproduce, for the purpose of preservation and making available to the public, including for addition to the DSpace digital archives until expiry of the term of validity of the copyright, and

1.2. make available to the public via the web environment of the University of Tartu, including via the DSpace digital archives until expiry of the term of validity of the copyright,

Prototype Design of ESTCube-2 Electrical Power System Control Electronics supervised by Mihkel Pajusalu and Erik Ilbis.

2. I am aware of the fact that the author retains these rights.

3. I certify that granting the non-exclusive licence does not infringe the intellectual property rights or rights arising from the Personal Data Protection Act.

Tartu, 22.05.2015